New Phytologist

Research

Xylan glucuronic acid side chains fix suberin-like aliphatic compounds to wood cell walls

Marta Derba-Maceluch[1], Madhusree Mitra[1], Mattias Hedenström[2], Xiaokun Liu[1], Madhavi L. Gandla[2], Félix R. Barbut[1], Ilka N. Abreu[1], Evgeniy N. Donev[1], János Urbancsok[1], Thomas Moritz[1], Leif J. Jönsson[2], Adrian Tsang[3], Justin Powlowski[3†], Emma R. Master[4] and Ewa J. Mellerowicz[1]

[1]Department of Forest Genetics and Plant Physiology, Umeå Plant Science Centre, Swedish University of Agricultural Sciences, 901 83 Umeå, Sweden; [2]Department of Chemistry, Umeå University, 901 87 Umeå, Sweden; [3]Centre for Structural and Functional Genomics, Concordia University, Montreal, QC H4B 1R6, Canada; [4]Department of Chemical Engineering and Applied Chemistry, University of Toronto, 200 College Street, Toronto, ON M5S 3E5, Canada

Author for correspondence:
Ewa J. Mellerowicz
Email: *ewa.mellerowicz@slu.se*

Received: *10 October 2022*
Accepted: *30 November 2022*

New Phytologist (2023) **238:** 297–312
doi: 10.1111/nph.18712

Key words: lignin–carbohydrate complexes, *Populus*, saccharification, suberin, wood cell wall, xylan.

Summary

- Wood is the most important repository of assimilated carbon in the biosphere, in the form of large polymers (cellulose, hemicelluloses including glucuronoxylan, and lignin) that interactively form a composite, together with soluble extractives including phenolic and aliphatic compounds. Molecular interactions among these compounds are not fully understood.
- We have targeted the expression of a fungal α-glucuronidase to the wood cell wall of aspen (*Populus tremula* L. × *tremuloides* Michx.) and Arabidopsis (*Arabidopsis thaliana* (L.) Heynh), to decrease contents of the 4-*O*-methyl glucuronopyranose acid (mGlcA) substituent of xylan, to elucidate mGlcA's functions.
- The enzyme affected the content of aliphatic insoluble cell wall components having composition similar to suberin, which required mGlcA for binding to cell walls. Such suberin-like compounds have been previously identified in decayed wood, but here, we show their presence in healthy wood of both hardwood and softwood species. By contrast, γ-ester bonds between mGlcA and lignin were insensitive to cell wall-localized α-glucuronidase, supporting the intracellular formation of these bonds.
- These findings challenge the current view of the wood cell wall composition and reveal a novel function of mGlcA substituent of xylan in fastening of suberin-like compounds to cell wall. They also suggest an intracellular initiation of lignin–carbohydrate complex assembly.

Introduction

The walls of wood cells of trees are crucial sources of renewable biomass (Bar-On *et al.*, 2018) for producing fuels and chemicals or as a versatile material for solid wood products. Dried wood consists of *c.* 45% cellulose, 25% hemicelluloses, and other polysaccharide matrix components, 20% lignin, 7% extractives, and 3% ash, with wide variation within a tree, among different species of angiosperms, or as a result of environmental stresses. Several wood-chemical analyses have used different approaches to reveal intricate details of the nanostructure of wood (Terashima *et al.*, 2009; Fernandes *et al.*, 2011; Bar-On *et al.*, 2018; Lyczakowski *et al.*, 2019; Terrett *et al.*, 2019; Addison *et al.*, 2020), with the results suggesting that wood properties are largely determined by molecular interactions among different wood components. Hemicelluloses play a unique role in these interactions by mediating the contact between the rigid semicrystalline cellulose microfibril network and the more flexible lignin network (Berglund *et al.*, 2020). Hemicelluloses coat cellulose hydrophobic and hydrophilic microfibril surfaces according to the presence and distribution of their side chains (Bromley *et al.*, 2013; Busse-Wicher *et al.*, 2014, 2016; Grantham *et al.*, 2017; Martínez-Abad *et al.*, 2017, 2020) and closely interact with lignin at the subnano scale (Kang *et al.*, 2019; Addison *et al.*, 2020) to form 'lignin–carbohydrate complexes' (LCCs; Tarasov *et al.*, 2018; Giummarella *et al.*, 2019; Terrett & Dupree, 2019).

In hardwoods, glucuronoxylan is the main hemicellulose. Its backbone, comprising β-1,4-linked D-Xyl*p* units, favors a threefold screw conformation in solution, but acquires a twofold conformation when interacting with cellulose microfibrils, which requires even spacing of xylan side chains: *O*-acetyl groups at position *O*-2, *O*-3, or both, and 4-*O*-methyl glucuronopyranose acid (mGlcA) units linked by a 1,2-α-glycosidic bond (Busse-Wicher *et al.*, 2014, 2016; Grantham *et al.*, 2017). The major xylan domain is characterized by even side-group spacing, while the minor domain has tight and uneven glucuronosylation and

†Deceased.

© 2023 The Authors
New Phytologist © 2023 New Phytologist Foundation
This is an open access article under the terms of the Creative Commons Attribution-NonCommercial-NoDerivs License, which permits use and distribution in any medium, provided the original work is properly cited, the use is non-commercial and no modifications or adaptations are made.

acetylation patterns (Busse-Wicher *et al.*, 2014). Both domains can represent different parts of the same or separate molecules and are formed by different xylan glucuronosyl and acetyltransferases (Bromley *et al.*, 2013; Grantham *et al.*, 2017). The minor domain is more difficult to extract because it interacts covalently with lignin (Martínez-Abad *et al.*, 2018).

Glucuronoxylan mediates three main LCCs: phenyl glycosides, linking phenolic C-4 to Xyl*p* C1-*O*; γ-esters, linking lignin unit γ-carbon to the mGlcA carboxyl group (C6-*O*); and benzyl ethers, linking lignin unit α-carbon to C2-*O* or C3-*O* in Xyl*p* (Tarasov *et al.*, 2018; Giummarella *et al.*, 2019; Terrett & Dupree, 2019). In birch, γ-esters and benzyl ether linkages are found in the highly recalcitrant fraction, whereas phenyl glycosidic LCCs are easily extracted (Martínez-Abad *et al.*, 2018). Molecular dynamic simulations suggested that mGlcA side chains may interact ionically with Ca^{2+} forming intermolecular cross-links analogous to the pectin egg-box structures (Pereira *et al.*, 2017). Thus, the presence and distribution of mGlcA substitutions in xylan are predicted to play crucial roles in determining the cell wall properties of hardwoods.

To assess the molecular implications of mGlcA substitution, we and others examined mutants of xylan glucuronosyl transferases, which form a small clade in the glycosyl transferase family 8 (GT8), and are encoded by *GUX1–GUX5* in *Arabidopsis thaliana* (Mortimer *et al.*, 2010, 2015; Lee *et al.*, 2012; Rennie *et al.*, 2012; Bromley *et al.*, 2013). Recently, similar genes have been described for conifers (Lyczakowski *et al.*, 2021). GUX1 and GUX3 generate an even glucuronosylation pattern, typically every eighth or sixth Xyl*p*, respectively, while GUX2 generates an uneven and consecutive glucuronosylation pattern. Therefore, single, double, and triple mutants of these genes display precise changes in mGlcA patterns in *A. thaliana*. The triple-mutant *gux1gux2gux3* is a dwarf, but the *gux1gux2* mutant grows normally despite the reduced level of xylan glucuronosylation. During saccharification, these plants have moderately and greatly increased glucose and xylose yields, respectively (Lee *et al.*, 2012; Lyczakowski *et al.*, 2017). However, the reduced glucuronosylation increases xylan acetylation because the two substituents compete for the same sites in xylan (Chong *et al.*, 2014; Lee *et al.*, 2014). Moreover, the suppressed GUX activity likely alters substrate pool in the Golgi, resulting in an increase cell wall Xyl content (Lee *et al.*, 2014; Chong *et al.*, 2015). Therefore, the cell wall and lignocellulose properties of the *gux* mutants are likely to be affected by other factors in addition to the change in mGlcA substitution.

To reduce xylan glucuronosylation without introducing additional structural changes, we previously expressed an α-glucuronidase of *Schizophyllum commune Sc*AGU115 in *A. thaliana* targeting it to the cell wall (Chong *et al.*, 2015). *Sc*AGU115 belongs to a novel α-glucuronidase family GH115 that acts on polymeric xylan (Tenkanen & Siika-aho, 2000), but *in planta*, it was active only on a small population of mGlcA residues that were accessible to UX1 monoclonal antibody (Chong *et al.*, 2015). The UX1 antibody binds GlcA decorations on deacetylated xylan (Koutaniemi *et al.*, 2012). As the majority of Xyl*p* units decorated by mGlcA are acetylated in native glucuronoxylan (Chong *et al.*, 2014), prior deacetylation of the xylan would be necessary for hydrolysis of mGlcA by *Sc*AGU115. Here, we used instead an α-glucuronidase of *Aspergillus niger* (*An*Agu67A) from the family GH67 representing enzymes that remove glucuronosyl residue from terminal nonreducing end of xylo-oligosaccharides (Tenkanen & Siika-aho, 2000), and we targeted it to the cell walls of hybrid aspen (*Populus tremula* L. × *tremuloides* Michx.) and *A. thaliana*. This uncovered previously unrecognized functions of xylan glucuronosylation in the wood and has led to identification of a novel wood component.

Materials and Methods

Gene cloning and recombinant expression of *AnAgu67A*

The cDNA clone Asn_01446 (GenBank accession: DR701927.1) encoding α-glucuronidase of *Aspergillus niger* Tiegh. (hereinafter *AnAgu67A*) was isolated as part of a fungal species gene discovery program (GenBank BioSample: SAMN00176483; EST: LIBEST_017623), where Q96WX9 and NRRL3_01069 are other identifiers of the same gene. For recombinant expression, *AnAgu67A* cDNA was amplified by PCR and transferred to ANIp7G (Storms *et al.*, 2005) using Gateway LR Clonase™ (Invitrogen). The details of cloning are presented in Supporting Information Methods S1. Enzyme activity assays of recombinant *An*Agu67A are described in Methods S2.

Plant vector construction

The *A. niger* α-glucuronidase cDNA clone Asn_01446 (GenBank accession: DR701927.1) was used to create a plant expression vector. The native signal peptide sequence was exchanged to the plant signal peptide from the *PtxtCel9B3* gene (alias *PttCel9B*) from *P. tremula* L. × *tremuloides* Michx. (GenBank accession no. AY660968.1; Rudsander *et al.*, 2003) with use of the following primers: OC9Bf1, OC9Br1, FC1f1, FC1r1, and FC1r1s (Table S1) as described previously (Gandla *et al.*, 2015). The entry clone was created using the pENTR/D-TOPO cloning system (Thermo Fisher Scientific, Uppsala, Sweden), and the expression clone was obtained using the Gateway®System (Thermo Fisher Scientific) in either the pK2WG7.0 vector (Karimi *et al.*, 2002) for overexpression using the 35S promotor in hybrid aspen or pK-pGT43B-GW7 (Ratke *et al.*, 2015) for expression specifically in cells developing secondary cell walls in *A. thaliana*. The destination vector pK7FGW2.0 was used to fuse $SP_{PttCel9B}$:AnAgu67A with GFP (Karimi *et al.*, 2002). All plant vectors were introduced into competent *Agrobacterium tumefaciens* (Smith and Townsend) Conn strain GV3101 using electroporation.

Plant material transformation and growth conditions

Hybrid aspen (*P. tremula* L. × *tremuloides* Michx., clone T89) was transformed by *A. tumefaciens* and propagated *in vitro* as described previously (Gray-Mitsumune *et al.*, 2008). Five lines with the highest *AnAgu67A* expression were selected out of the 23 analyzed lines. Between nine and 13 trees of each of the five selected lines and 19 wild-type (WT) trees were grown in a

© 2023 The Authors
New Phytologist © 2023 New Phytologist Foundation

14698137, 2023, 1, Downloaded from https://nph.onlinelibrary.wiley.com/doi/10.1111/nph.18712 by Swedish University Of Agricultural Sciences, Wiley Online Library on [24/04/2023]. See the Terms and Conditions (https://onlinelibrary.wiley.com/terms-and-conditions) on Wiley Online Library for rules of use; OA articles are governed by the applicable Creative Commons License

glasshouse for 3 months as described previously (Gandla *et al.*, 2015). The stem height, the average internode length for internodes 19–35, and the stem diameters for internode 40 were determined at the time of harvest.

Arabidopsis thaliana (L.) Heynh (Col-0) was transformed using the floral dip method (Clough & Bent, 1998). Seeds collected from the transformed plants were germinated on ½ Murashige & Skoog medium (½ MS) plates with kanamycin (50 μg ml^{-1}) and homozygotic single insert lines were selected by segregation. Plants of the two highest expressing lines were grown for 8 wk under a 16 h : 8 h, light : dark cycle, 150 μmol m^{-2} s^{-1}, at 22°C and 70% humidity.

Immunolocalization of $SP_{PttCel9B}$:AnAgu67A:GFP

T2 *A. thaliana* seeds carrying the transgene were germinated on ½ MS plates, and 7-d-old seedlings were plasmolyzed in 20% mannitol, fixed in 2% w/v paraformaldehyde, and used for immunolocalization as described previously (Pawar *et al.*, 2016), except that the Cy™5 AffiniPure Donkey Anti-Rabbit IgG (H + L; Jackson ImmunoResearch Europe Ltd, Ely, UK) diluted 1 : 200 was used as secondary antibody. The seedling roots were analyzed by sequential line scanning using a Leica TCS SP2 confocal microscope with 633 nm excitation and 650–798 nm emission (Leica Microsystems, Wetzlar, Germany). The lambda scan was performed every 6 nm between 650 and 800 nm to ensure that the signal matched that of Cy5.

qRT-PCR analysis

RNA was isolated from developing xylem tissues of hybrid aspen as previously described (Gray-Mitsumune *et al.*, 2004) using CTAB buffer (Chang *et al.*, 1993), before being treated with DNaseI (DNA-free™ DNA Removal Kit; Thermo Fisher Scientific). The cDNA library was made from 1 μg of RNA using an iScript™ cDNA Synthesis Kit (Bio-Rad Laboratories AB, Hercules, CA, USA), and cDNA diluted 1 : 20 was used for transcript-level analysis. The expression was normalized to tubulin (*Potri.001G464400*) and ubiquitin (*Potri.005G198700*), calculated according to Pfaffl (2001) and presented relative to the lowest-expressing line.

In the case of *A. thaliana*, RNA was isolated from the stems of 6-wk-old plants using TRI Reagent® (Applied Biosystems, Bedford, MA, USA). The cDNA libraries were made as described previously from 400 ng of RNA and diluted 10 times for transcript-level analysis. The expression was calculated according to Livak & Schmittgen (2001), was normalized to *ACTIN2* (*AT3G18780*) and *EF1ALPHA* (*AT5G60390*), and presented relative to the lowest-expressing line. The primers details are provided in Table S1.

Alpha-glucuronidase activity assay in transgenic plants

Portions of 100 mg of either developing wood, in the case of hybrid aspen, or stem tissues, in the case of *A. thaliana*, were ground in liquid nitrogen, incubated in 300 μl of buffer A (0.2 M sodium succinate, pH 5.5), 10 mM $CaCl_2$, and 1% (w/v) PVPP (aspen) or 1% (w/v) PVP (*A. thaliana*) at 4°C for 1 h with shaking, spun at 20 000 ***g*** for 15 min, and the supernatants were collected as soluble protein fractions. The pellets were extracted with 200 μl of buffer B (0.2 M sodium succinate, 10 mM $CaCl_2$, and 1 M NaCl, pH 5.5) for 1 h at 4°C with shaking, spun as above, and the supernatans were collected as wall-bound protein fractions, which were desalted using Microcon centrifugal filters (30 000 MWCO; Millipore) and equilibrated in buffer A. The protein concentrations were determined by the Bradford method and adjusted to 0.3 and 0.59 mg ml^{-1} for hybrid aspen and *A. thaliana*, respectively.

The α-glucuronidase activity assay was performed using the K-AGLUA Assay Kit (Megazyme, currently Neogen Europe Ltd, Ayr, UK) using 7.5 μg of proteins from soluble and wall-bound fractions for hybrid aspen, and 14.75 μg of protein from the wall-bound fraction for *A. thaliana* according to manufacturer's instructions. Briefly, the proteins were incubated with a mixture of tri-, tetra-, and penta-aldouronic acid (provided in the kit) for 20 min of a two-step reaction at 40°C, where the α-glucuronidase product (glucuronic acid) was further reacted with nicotinamide adenine dinucleotide (NAD^+) to form D-glucarate and reduced NADH that was spectrophotometrically measured at 340 nm.

Thin-layer chromatography analysis was used to visualize the α-glucuronidase reaction in hybrid aspen according to Franková & Fry (2011). Details are presented in Methods S3.

Anatomy

Stem segments from internode 42 of hybrid aspen were fixed in FAA (50% ethanol, 4% formaldehyde, 5% acetic acid; v/v/v). Fifty micrometer-thick transverse sections were cut using a vibratome (VT100S; Leica Biosystems) and stained with Mäule reagent (Meshitsuka & Nakano, 1977). Sections were incubated in 1% (w/v) $KMnO_4$ for 5 min, washed three times with distilled water, and incubated in 37% N HCl for 2 min. The stained sections were mounted in the presence of concentrated NH_4OH and observed under a Dmi8 microscope (Leica Microsystems) in white light with a color DCF7000 T camera. Thicknesses of secondary xylem, secondary phloem, and bark were analyzed in three trees per line.

Suberin localization

Stem sections prepared as above were stained with Fluorol Yellow 088 (FY088; Lux *et al.*, 2005) either directly or after prior removal of soluble extractives as described below. Unstained sections were used as control for lignin autofluorescence. Sections were examined with a Dmi8 microscope using standard GFP settings (excitation, 450–490 nm; dichroic mirror, 495; emission 500–550 nm) and a monochromatic camera DCF9000 GT. Fluorescence was quantified using LasX software (Leica Microsystem CMS GmbH) in the line mode. Three trees were analyzed per genotype, using 3–19 images per tree, and the fluorescence signal was measured at a minimum of 15 positions per image and averaged. The staining and imaging settings were consistent across the lines and treatments that were compared.

© 2023 The Authors
New Phytologist © 2023 New Phytologist Foundation

14698137, 2023, 1, Downloaded from https://nph.onlinelibrary.wiley.com/doi/10.1111/nph.18712 by Swedish University Of Agricultural Sciences, Wiley Online Library on [24/04/2023]. See the Terms and Conditions (https://onlinelibrary.wiley.com/terms-and-conditions) on Wiley Online Library for rules of use; OA articles are governed by the applicable Creative Commons License

Wood grinding for compositional analysis

Hybrid aspen internodes 44–60 were debarked and freeze-dried for 36 h. The pith was removed, and the wood was milled using an A11 Basic Analytical Mill (IKA, Staufen, Germany) followed by grinding in a ZM 200 ultra centrifugal mill (Retsch, Haan, Germany). Rough wood powder (particle size < 0.5 mm) was further milled to a fine wood powder in 10-ml stainless steel jars with one 12-mm grinding ball at 30 Hz for 2 min, using an MM400 bead mill (Retsch).

Pyrolysis coupled to gas chromatography/mass spectrometry (Py-GC/MS)

Portions of 50 ± 10 µg of fine wood powder were applied to a pyrolyzer equipped with an autosampler (PY-2020iD and AS-1020E; Frontier Lab, Koriyama, Japan) connected to a GC/MS (7890A/5975C; Agilent Technologies AB, Santa Clara, CA, USA), and the pyrolysate was separated and analyzed according to Gerber *et al.* (2012).

FT-IR spectroscopy

Samples of fine wood powder (10 mg) were analyzed as described previously (Gandla *et al.*, 2015) using a Bruker IFS 66v/S spectrometer (Bruker Optik GmbH, Ettlingen, Germany) equipped with a diffuse reflectance 16-sample holder accessory (Harrick Scientific Products, Pleasantville, NY, USA). Samples of 9–13 trees of each transgenic line and 19 WT trees were examined.

Wood wet chemistry analyses

The fine wood powders of two trees of the same line were pooled to provide 4–5 biological replicates per line. The alcohol insoluble residue (AIR) was prepared by washing the samples with 4 mM HEPES buffer (pH 7.5) containing 80% ethanol, a methanol : chloroform 1 : 1 (v/v) mixture, and finally with acetone, before drying the residue in a vacuum (Gandla *et al.*, 2015). Type I α-amylase from pig pancreas (Roche, Solna, Sweden: 10102814001; 100 U/100 mg of AIR) was used to remove starch from AIR following two overnight incubations with fresh addition of the enzyme each day.

Methanolysis-TMS analysis was conducted using 500 µg of either starch-free AIR material or dioxane lignin isolated as described below, together with inositol (10 µg; internal standard) and nine monosaccharide standards, as described previously (Gandla *et al.*, 2015). Silylated monosaccharides were separated by GC/MS (7890A/5975C; Agilent Technologies AB). The resulting raw data MS files were converted to CDF format in Agilent Chemstation Data Analysis (v.E.02.00.493) and exported to R software (v.3.0.2; R Foundation for Statistical Computing). Data pretreatment procedures, such as baseline correction and chromatogram alignment, time-window setting, and multivariate curve resolution (MCR) processing, followed by peak identification were performed in R, and 4-O-methylglucuronic acid was identified according to Chong *et al.* (2013).

The crystalline cellulose content was determined by the Updegraff procedure (Updegraff, 1969), the resulting glucose content was determined using the anthrone method as previously described (Gandla *et al.*, 2015), and the acid-insoluble lignin (Klason lignin) content was determined according to Theander & Westerlund (1986).

Analytical saccharification

Each line was analyzed with four or five biological replicates, each representing a pool of wood powder (particle size: 0.1–0.5 mm) from two trees obtained by fractionation of the rough wood powder using an AS 200 analytical sieve shaker (Retsch). Moisture content in 50 mg wood powder samples was measured using Mettler Toledo HG63 moisture analyzer (Columbus, OH, USA). The acid pretreatment, enzymatic saccharification, and resulting hydrolysate analyses were conducted as previously described previously (Gandla *et al.*, 2015). Briefly, the acid pretreatment was performed in 1% (w/w) sulfuric acid for 10 min at 165°C using an initiator single-mode microwave instrument (Biotage Sweden AB, Uppsala, Sweden). The enzymatic hydrolysis after acid pretreatment was performed at 45°C for 72 h in sodium citrate buffer (50 mM, pH 5.2) using 50 mg of an enzyme mix of Celluclast 1.5 l and Novozyme 188 (1 : 1, obtained from Sigma–Aldrich (St Louis, MO, USA)), in a reaction mixture of 1000 mg. Reaction mixtures with wood that had not been pretreated consisted of 50 mg of milled wood, 900 mg of the sodium citrate buffer, and 50 mg of the same enzyme mix. The yield of Glc and Xyl was determined following the method as mentioned by Gandla *et al.* (2015) using a high-performance anion-exchange chromatography system with pulsed amperometric detection (Ion Chromatography System ICS-3000 by Dionex, Sunnyvale, CA, USA).

Dioxane-lignin isolation

Fractionated wood powder (particle size: 0.1–0.5 mm) was pooled from nine trees to obtain a single sample of ≥ 7.5 g. Materials from nine transgenic trees, including three trees each from lines 4, 6, and 23, and nine WT trees were pooled equally by weight to obtain one transgenic and one WT sample. Part of the material (extracted wood) was extracted sequentially in three technical replicates in a Soxhlet apparatus for 6 h with toluene (95% EtOH; 2 : 1; v/v), for 4 h in 95% EtOH, and for 2 h in H_2O, and finally, the extracted wood was dried in an oven at 103°C for 48 h (this step was omitted for nonextracted samples). The material was ground in 0.3–1.2 g portions in a Planetary Micro Mill Pulverisette 7 Premium line (Fritsch, Idar-Oberstein, Germany) with 10 ZrO_2 balls (10-mm diameter) at 500 rpm over five 10-min milling cycles, with a 10-min break between each. The finely ground material was suspended in 1,4-dioxane : water (96 : 4; v/v) with a solid : liquid ratio of 1 : 10 (g ml^{-1}) and shaken at 225 rpm for 24 h at room temperature. The suspension was centrifuged at 4000 ***g*** for 10 min, the supernatant was collected, and the pellet was re-extracted with 1,4-dioxane : water a further three times. The four extractions were

© 2023 The Authors
New Phytologist © 2023 New Phytologist Foundation

14698137, 2023, 1, Downloaded from https://nph.onlinelibrary.wiley.com/doi/10.1111/nph.18712 by Swedish University Of Agricultural Sciences, Wiley Online Library on [24/04/2023]. See the Terms and Conditions (https://onlinelibrary.wiley.com/terms-and-conditions) on Wiley Online Library for rules of use; OA articles are governed by the applicable Creative Commons License

combined and filtered through a Whatman glass microfiber filter (pore size 1.2 µm; Merck, Solna, Sweden), following which, two volumes of water were added to precipitate the lignin–carbohydrate mixture. The 1,4-dioxane and water were evaporated in a rotary evaporator (under reduced pressure) at 35°C to almost dryness, before adding 10 ml of water and evaporating again to almost dryness; this process was repeated three times to remove 1,4-dioxane. Finally, 10 ml of water was added to the sample, transferred to a Falcon tube, and lyophilized in a freeze-dryer for 24 h to obtain 'dioxane lignin'.

NMR

Dioxane lignin (10–15 mg) was transferred to 5-mm NMR tubes and dissolved in 600 ml dimethyl sulfoxide-d_6 (Kim *et al.*, 2008). 2D ^{1}H-^{13}C heteronuclear single quantum coherence (HSQC) profiles were acquired at 298 K using a Bruker 600 MHz Avance III spectrometer equipped with a 5 mm BBO cryo-probe (Bruker Biospin, Rheinstetten, Germany). A pulse program employing adiabatic ^{13}C refocusing and inversion pulses was used (hsqcetgpsisp2.2), with sweep widths of 8.1 ppm in the ^{1}H dimension and 140 ppm in the ^{13}C dimension. Sixteen scans were recorded for each of the 256 t_1 increments, and the spectra were calibrated using the residual dimethyl sulfoxide peak (d_H: 2.49 ppm and d_C: 39.5 ppm). A Gaussian window function was used in F1 (^{13}C dimension), and a 90-degree shifted square sine bell window function was applied in F2 (^{1}H dimension). Processing and peak volume integration were performed in Topspin 3.6 (Bruker Biospin), and peak assignments were based on those used in previous studies (Kim *et al.*, 2008; Balakshin *et al.*, 2011; Shakeri Yekta *et al.*, 2019; Correia *et al.*, 2020). Orthogonal partial least square (OPLS) analysis and visualization were performed using an in-house MATLAB application that transforms a batch of 2D spectra to a matrix suitable for multivariate analysis by reshaping each spectrum to a row vector (Hedenström *et al.*, 2009; Öman *et al.*, 2014).

Metabolomic analysis

Metabolites were extracted and analyzed as described by Abreu *et al.* (2020). Briefly, 20 mg of fine wood powder was extracted in 1 ml of extraction buffer (methanol : chloroform : water; 20 : 60 : 20; v/v/v), including internal standards (Gullberg *et al.*, 2004), and 100 µl of each extract was dried in a SpeedVac and dissolved in 20 µl of methanol followed by 20 µl of water. Lipids were extracted in methanol : chloroform (50 : 50, v/v) as described by Melo *et al.* (2021). Metabolomics and lipidomics analyses were performed by liquid chromatography, and the metabolites were detected by an Agilent 6540 Q-TOF mass spectrometer equipped with an electrospray ion source operating in negative and/or positive ion modes (Abreu *et al.*, 2020). The mass files from the metabolomic analysis were processed (Profinder B.08.00; Agilent Technologies AB) by a targeted feature extraction approach using the aspen stem database (Abreu *et al.*, 2020), while those from the lipidomic analysis were processed by an untargeted approach using a recursive feature extraction as described by Melo *et al.* (2021). The generated data were normalized against the internal standard and weight of each sample. The targeted approach used to process phenolic compounds resulted in the annotation of 135 metabolites (Table S5, see later), which was confirmed by comparison of MS fragments (produced by MS/MS analysis) with the results of previous studies (Kasper *et al.*, 2012; Abreu *et al.*, 2020). Annotation was performed on significant ion mass. The untargeted approach used for the lipid MS files resulted in the detection of 984 (positive) and 980 (negative) features. Lipid compounds were annotated based on mass spectra in the library LIPIDMAPS (https://www.lipidmaps.org/). Changes in abundance between transgenic and WT samples were considered as significant if $P \leq 0.05$ (*t*-test) and, in the case of lipids, |fold change| ≥ 1.5. The false discovery rate was < 0.05.

Transcriptomics

RNA samples were isolated from developing wood, and their concentrations were determined by a NanoDrop 2000 spectrophotometer (Thermo Fisher Scientific). The quality of the RNA was assessed by an Agilent 2100 Bioanalyzer (Agilent Technologies AB) following the manufacturer's instructions, and samples with an integrity number (RIN) ≥ 8 were used for sequencing. Four biological replicates of line 4, three biological replicates of line 6, and eight biological replicates of WT were analyzed. Sequencing was conducted by Novogene (Cambridge, UK) using an Illumina NovaSeq 6000 PE150 platform, as was the quality control and mapping to the *P. tremula* transcriptome v.2.2 (retrieved from PlantGenIE; ftp://plantgenie.org/Data/PopGenIE/Populus_tremula/v2.2/). The raw counts were used for differential expression analysis in R (v3.4.0) using the BIOCONDUCTOR (v.3.4) DESEQ2 package (v.1.16.1) as previously described (Kumar *et al.*, 2019).

Statistical analyses

Univariate analyses were conducted using JMP v.15.0.0. program (SAS Institute). SIMCA-P software (v.16.0.1; Sartorius Stedim Data Analysis AB, Goettingen, Germany), with built-in options, was used for multivariate analysis.

Results

Production of *An*Agu67A

The recombinant *An*Agu67A protein purified from *A. niger* exhibited α-glucuronidase activity, and a half-life of > 2 h at 40°C and *c.* 1 h at 60°C. Hydrolysis of aldouronic acids by *An*Agu67A was optimal at pH 5.0 and between 50°C and 60°C (Fig. S1a,b); the k_{cat} and K_m of *An*Agu67A were 4.6×10^{-2} s^{-1} and 3.5 mg ml^{-1}, respectively. Two pure aldouronic acid fractions were tested as *An*Agu67A substrates: UXX, with an mGlcA substituent on the terminal nonreducing end of xylotriose; and XUXX, with an mGlcA substituent at the second Xyl*p* unit from the nonreducing end of xylotetraose. Consistent with the

© 2023 The Authors
New Phytologist © 2023 New Phytologist Foundation

14698137, 2023, 1, Downloaded from https://nph.onlinelibrary.wiley.com/doi/10.1111/nph.18712 by Swedish University Of Agricultural Sciences, Wiley Online Library on [24/04/2023]. See the Terms and Conditions (https://onlinelibrary.wiley.com/terms-and-conditions) on Wiley Online Library for rules of use; OA articles are governed by the applicable Creative Commons License

substrate preferences of the GH67 family, mGlcA was released from the UXX substrate only (Chong *et al.*, 2015). mGlcA was also released from birchwood xylan by the recombinant enzyme (Fig. S2c), indicating that terminal mGlcA decorations at the reducing end are present in native wood xylan.

Ectopically expressed *AnAgu67A*-induced reduction in mGlcA xylan branching has no significant effects on the aspen growth phenotype, wood composition, or saccharification

A chimeric gene was cloned by substituting the *AnAgu67A* signal peptide with the signal peptide of *Ptxt*Cel9B3 (SP_{Cel9B3}) for efficient targeting of the fungal enzyme to the plant cell wall. To verify the proper targeting, the chimeric gene was fused to e*GFP* and *35S::*SP_{Cel9B3}*:AnAgu67A:eGFP* construct was transferred to *A. thaliana*. As expected, the fusion protein was localized in cell walls in plasmolyzed root cells (Fig. 1a). Transgenic hybrid aspen lines were subsequently produced using the *35S::*SP_{Cel9B3}*:AnAgu67A* construct (*AnAgu67A* lines or transgenic lines) and grown in a glasshouse. The transgene was found expressed in developing wood in all analyzed lines (Fig. 1b), with the lowest expression in line 9, which was therefore omitted in some analyses.

As plants do not have endogenous α-glucuronidase activity, we examined α-glucuronidase activity in wall-bound protein extracts of developing wood from transgenic plants (Fig. 1c). The extracts of all analyzed transgenic lines hydrolyzed UXX to xylotriose and mGlcA, as was observed for *An*Agu67A protein *in vitro*, whereas no activity was detected in the WT (Fig. 1c). Quantitative analysis of α-glucuronidase activity in the soluble and wall-bound protein fractions extracted from the developing wood of transgenic lines showed predominant activity in the wall-bound fraction (Fig. 1d) in agreement with protein localization to the cell wall and was the highest in lines 4 and 6.

The effects of α-glucuronidase activity on the sugar composition of wood matrix polysaccharides were investigated by methanolysis-trimethylsilyl (TMS) derivatization. A 20–30% reduction in mGlcA units was evident in all transgenic lines except for the low-expressing line 9, while no changes were observed in other sugar-related constituents (Figs 1e, S2a). The wood chemistry was analyzed by pyrolysis-GC/MS (Py-GC/MS), Fourier-transform infrared spectroscopy (FT-IR), Updegraff cellulose analysis, and Klason lignin, with no significant changes observed compared with WT (Fig. S2b–e).

To examine the effects of 20–30% reduction in xylan glucuronosylation on saccharification, wood from transgenic lines with reduced mGlcA was analyzed by analytical enzymatic saccharification with and without acid pretreatment. The results showed no significant change in glucose or xylose release in the transgenic lines compared with WT (Fig. S2f–g), which contrasts with the previously reported improved saccharification in *gux1gux2* and *gux1gux2gux3* mutants (Lee *et al.*, 2012; Lyczakowski *et al.*, 2017).

The morphology and anatomy of transgenic trees were analyzed to determine whether the reduced xylan glucuronosylation affected plant growth and development, but the only change was a small but consistent decrease in stem height caused by a decreased internode length (Fig. 1f–h), which might indicate a role of xylan glucuronosylation in stem elongation. Otherwise, no major or consistent changes in stem radial growth or stem anatomy were detected among the analyzed transgenic lines (Fig. S3a–c).

Cell wall-localized AnAgu67A α-glucuronidase does not affect γ-linkages

As (m)GlcA substituents of xylan are involved in cross-linking xylan to lignin via γ-ester bonds, we tested whether the α-glucuronidase activity in cell walls impacted γ-ester bonds in LCCs, which can be solubilized from cell walls together with lignin using dioxane (Giummarella *et al.*, 2019). Dioxane-soluble lignin was isolated from transgenic and WT extractive-free wood samples and analyzed by Py-GC/MS. It was found to comprise *c.* 65% lignin and 35% carbohydrates in both transgenic and WT samples (Fig. S4a). Xylose was the main sugar unit of dioxane lignin, reaching *c.* 95 mole % in both transgenic and WT samples (Fig. S4b). In agreement with these results, 2D HSQC NMR analysis with peak quantification normalized to lignin aromatic units (Tarasov *et al.*, 2018) showed no significant differences between transgenic and WT samples in either different lignin signals or anomeric signals from xylan (Fig. S4c–e). Therefore, the LCC composition does not differ significantly between transgenic and WT trees. The γ-ester peak, which is in the *O*-alkylated region, was well resolved (Fig. S5), and its integrated signal constituted *c.* 6% and 7% of total lignin aromatic signals for WT and transgenic samples, respectively (Fig. S4d), which is close to the 5.6% previously reported for birch (Tarasov *et al.*, 2018). Thus, α-glucuronidase activity in cell walls did not impact the LCC composition nor the occurrence of γ-ester bonds.

AnAgu67A α-glucuronidase decreases the content of aliphatic compounds in dioxane lignin

The OPLS modeling of 2D HSQC NMR spectra of dioxane lignin from extractive-free wood of transgenic and WT samples (Fig. S5a,b) revealed the most significant changes between the two samples in the aliphatic region A, followed by the *O*-alkylated region B. The aromatic region C did not contribute to sample separation, which is consistent with the aromatic peak quantitative analysis (Fig. S4c). The high-resolution OPLS loading plots corresponding to regions A and B of the spectra are shown in Fig. 2(a,b). The loadings represent spectra that significantly contributed to the separation of transgenic and WT samples in OPLS. The blue signals, including aliphatic saturated and unsaturated esters, triacylglycerols (TAGs), and diacylglycerols (DAGs), were higher in WT, whereas all black peaks were higher in transgenic lines. Quantitative analysis of the integrated peaks normalized to lignin confirmed the reduced signals from fatty esters, TAGs, and DAGs in the dioxane lignin from transgenic plants from extractive-free wood samples, whereas the corresponding signals obtained from wood with extractives

© 2023 The Authors
New Phytologist © 2023 New Phytologist Foundation

14698137, 2023, 1, Downloaded from https://nph.onlinelibrary.wiley.com/doi/10.1111/nph.18712 by Swedish University Of Agricultural Sciences, Wiley Online Library on [24/04/2023]. See the Terms and Conditions (https://onlinelibrary.wiley.com/terms-and-conditions) on Wiley Online Library for rules of use; OA articles are governed by the applicable Creative Commons License

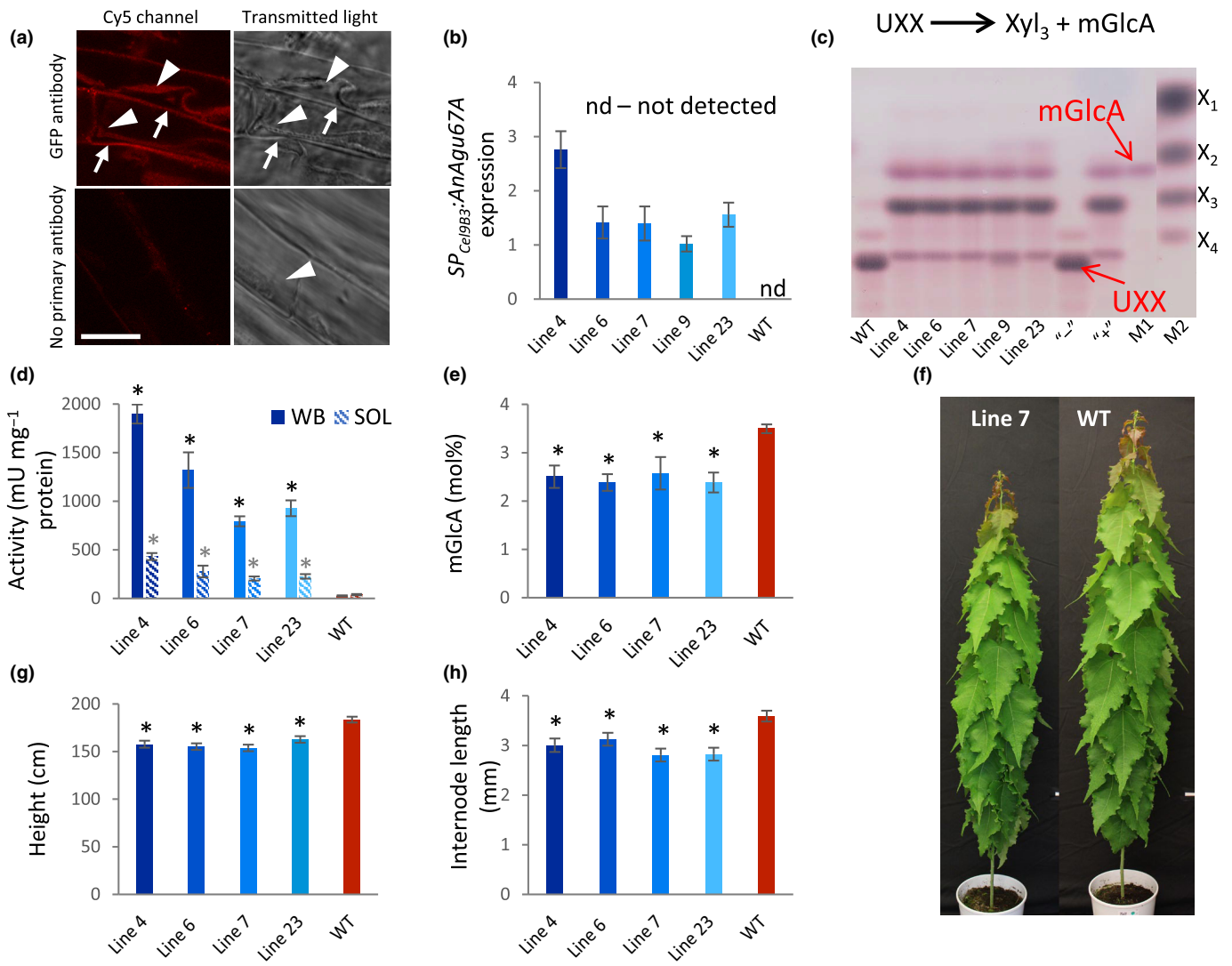

Fig. 1 Characterization of transgenic aspen (*Populus tremula* L. × *tremuloides* Michx.) lines carrying *35S::SP$_{Cel9B3}$:AnAgu67A* construct. (a) Immunolocalization of eGFP in plasmolyzed root cells of *Arabidopsis thaliana* expressing *35S::SP$_{Cel9B3}$: AnAgu67A:eGFP* showing that the protein is targeted to cell walls. Arrowhead, shrunken protoplast; arrow, *SP$_{Cel9B3}$: AnAguG7A:eGFP* signal in cell wall. Bar, 15 µm. (b) Relative expression of transgene in transgenic lines normalized to line 9. (c) Visualization of α-glucuronidase activity in wall-bound protein fractions extracted from developing wood of transgenic and wild-type (WT) lines showing products of UXX hydrolysis by thin-layer chromatography. M1 and M2 – size markers, '–' – negative control with buffer instead of protein extract, '+' – positive control with *Geobacillus stearothermophilus* Donk α-glucuronidase. (d) Specific activity of α-glucuronidase in soluble (SOL) and wall-bound (WB) protein fraction extracted from developing wood of transgenic and WT plants. (e) 4-*O*-MeGlcA reduction in transgenic lines detected in methanolysis-trimethylsilyl analysis. (f) Appearance of 10-wk-old trees. (g) Height. (h) Internode length. Data in (b), (d), (e), (g), and (h) are means ± SE of $n = 3$ (b), $n = 4$ (d, e), $n = 9$–19 (g, h), for 12-wk-old trees. Asterisks mark lines significantly different from WT at $P \leq 0.05$ (Dunnett's test).

(nonextracted wood) were similar for transgenic and WT samples (Fig. 2c). Therefore, *An*Agu67A affects the extractability of aliphatic compounds, but not their amounts in wood. This conclusion was consistent with the results of transcriptomic analyses of developing wood in transgenic aspen lines 4 and 6 that were most highly expressing *AnAgu67A* and in WT, which did not reveal any changes in expression of lipid-related genes (Table S2).

To identify the most highly extracted aliphatic compounds from wood of transgenic plants compared with WT, we analyzed both samples using untargeted lipidomics approach. Out of *c.* 1000 lipid peaks that were detected in the wood extracts (Table S3), 115 were significantly changed between transgenic and WT samples ($P \leq 0.05$ and fold change > 1.5). From the corresponding metabolites, 88 were annotated and classified into nine categories (Fig. 2d; Table S4); the majority (71/88) were increased in transgenic samples (Fig. 2d). Among the fatty acids (FAs) increased in the transgenic extracts, there were 13 suberin monomers, such as 5,9,23-triacontatrienoic acid (77-fold increase), 28-hydroxy-octacosanoic acid, 9-octadecenoic acid, suberic acid, and 9,10-epoxy-octadecanoic acid (Fig. 2d; Table S4). By contrast, three other suberin monomers, comprising tetradecanedioic acid, glutinic acid, and 2-hydroxy-heptanoic

© 2023 The Authors
New Phytologist © 2023 New Phytologist Foundation

14698137, 2023, 1, Downloaded from https://nph.onlinelibrary.wiley.com/doi/10.1111/nph.18712 by Swedish University Of Agricultural Sciences, Wiley Online Library on [24/04/2023]. See the Terms and Conditions (https://onlinelibrary.wiley.com/terms-and-conditions) on Wiley Online Library for rules of use; OA articles are governed by the applicable Creative Commons License

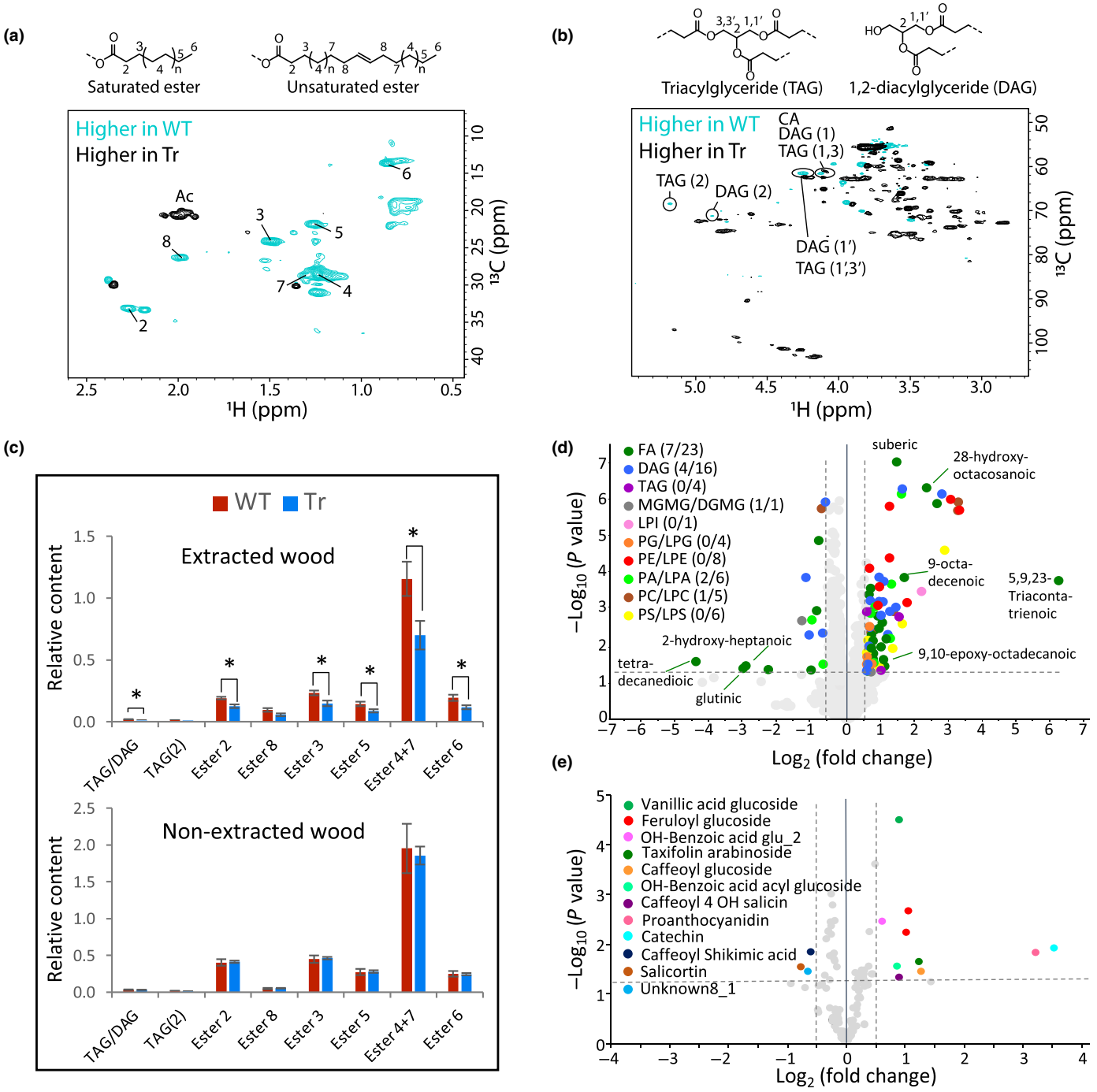

Fig. 2 Aliphatic suberin-like compounds are easier to extract from the wood of transgenic aspen (*Populus tremula* L. × *tremuloides* Michx.) expressing *AnAgu67A* (Tr) than from wild-type (WT) wood. Two-dimensional (2D) nuclear magnetic resonance spectra of dioxane-soluble lignin isolated after removal of extractives (extracted wood) in the aliphatic (a) and *O*-alkylated (b) spectral regions that contributed to separation of transgenic and WT samples in orthogonal projections to latent structures (OPLS) analysis. Details of the OPLS models for extracted and nonextracted wood and 2D signals from WT samples are shown in Supporting Information Fig. S5. Ac, acetate; CA, cinnamyl alcohol. (c) Quantitative analysis of integrated peaks from the aliphatic and *O*-alkylated regions of extracted and nonextracted wood. Means ± SE, $n = 3$ technical replicates of pooled material from three transgenic lines or from WT, asterisks show peaks significantly different between transgenic and WT samples at $P \leq 0.05$ (*t*-test). (d, e) Volcano plots showing aliphatic (d) and phenolic (e) metabolites extracted from the wood that differed in abundance between transgenic and WT samples ($P < 0.05$, *t*-test). The significantly altered metabolites are colored and represent in (d): DAG, diacylglycerols; FA, fatty acids; LPI, monoacylglycerophosphoinositols; MGMG/DGMG, (mono/di)glycosylmonoacylglycerols; PA/LPA, (di/mono)acylglycerophosphates; PC/LPC, (di/mono)acylglycerophosphocholines; PE/LPE, (di/mono)acylglycerophosphoethanolamines; PG/LPG, (di/mono)acylglycerophosphoglycerols; TAG, triacylglycerols; PS/LPS, (di/mono)acylglycerophosphoserines; (number of downregulated/upregulated metabolites). Cutin/suberin-related FAs are shown.

© 2023 The Authors
New Phytologist © 2023 New Phytologist Foundation

14698137, 2023, 1, Downloaded from https://nph.onlinelibrary.wiley.com/doi/10.1111/nph.18712 by Swedish University Of Agricultural Sciences, Wiley Online Library on [24/04/2023]. See the Terms and Conditions (https://onlinelibrary.wiley.com/terms-and-conditions) on Wiley Online Library for rules of use; OA articles are governed by the applicable Creative Commons License

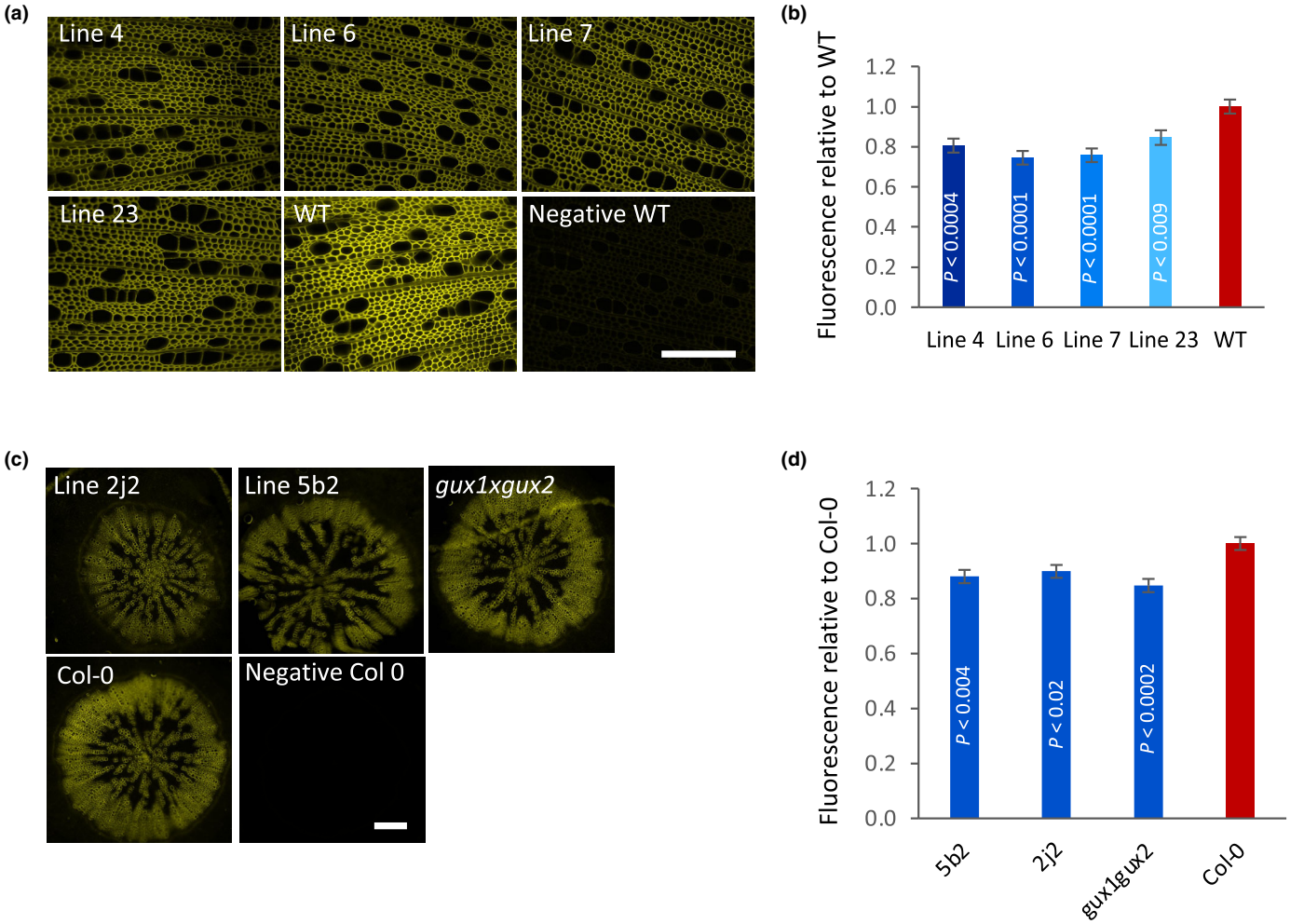

Fig. 3 Histochemical analysis of aliphatic compounds with FY088 in the wood of transgenic plants expressing *AnAgu67A* and wild-type (WT/Col0) after removal of extractives. (a) Representative sections of each line showing differences in suberin-like signals in 12-wk-old aspen (*Populus tremula* L. × *tremuloides* Michx.) stems. (b) Quantification of fluorescence signals in cell walls: means ± SE of $n = 36$. (c) Representative images of signals in 4-wk-old *A. thaliana* hypocotyls in two transgenic lines 5b2 and 2j2, in *gux1gux2* mutant and Col-0. Sections of 12 plants per genotype were analyzed. (d) Quantification of fluorescence signals in cell walls: means ± SE, $n = 12$. *P* values in (b) and (d) correspond to Dunnett's test comparing each genotype to WT/Col-0. Bars, 200 μm. Negative control in (a) and (c) shows autofluorescence signals without FY088.

acid, were reduced in transgenic extracts compared with WT; these FAs were characterized by shorter chains compared with those with increased extractability in the transgenic plants. The generally higher abundance of lipids in transgenic extracts confirms the NMR results, showing that aliphatic compounds are easier to extract when α-glucuronidase *An*Agu67A is present in cell walls. The high contribution of suberin-related FAs to the extractability suggests that *An*Agu67A affects the solubility of such compounds in wood. As suberin contains phenolic compounds linked with aliphatic compounds, we also investigated whether extracted phenolic compounds are more abundant in transgenic samples. A targeted metabolomic approach revealed 135 annotated phenolic compounds (Table S5), among which, 10, including tannins and glycosylated derivatives of hydroxycinnamic acids (known suberin components; Bernards, 2002; Graça, 2010), were more abundant in transgenic samples (Fig. 2e; Table S6).

*An*Agu67A-sensitive aliphatic compounds are present in sapwood cell walls

To determine the location of α-glucuronidase-sensitive suberin-like compounds in wood, we stained extracted stem sections of transgenic and WT trees with Fluorol Yellow 088 (FY088), which stains suberin (Naseer *et al.*, 2012). The results showed strong yellow fluorescence signals in all lignified cell walls of mature WT wood (Fig. 3a). These extraction-resistant signals were visibly reduced in transgenic lines, which was confirmed by quantitative image analysis (Fig. 3a,b). By contrast, the nonextracted sections of transgenic plants had similar signal intensity to the nonextracted WT sections (Fig. S6a–c), suggesting that *An*Agu67A was responsible for the enhanced liberation of these cell wall aliphatic compounds by toluene-ethanol solvent.

To investigate whether *An*Agu67A had a similar effect on cell wall aliphatic compounds in other species, transgenic lines

© 2023 The Authors
New Phytologist © 2023 New Phytologist Foundation

14698137, 2023, 1, Downloaded from https://nph.onlinelibrary.wiley.com/doi/10.1111/nph.18712 by Swedish University Of Agricultural Sciences, Wiley Online Library on [24/04/2023]. See the Terms and Conditions (https://onlinelibrary.wiley.com/terms-and-conditions) on Wiley Online Library for rules of use; OA articles are governed by the applicable Creative Commons License

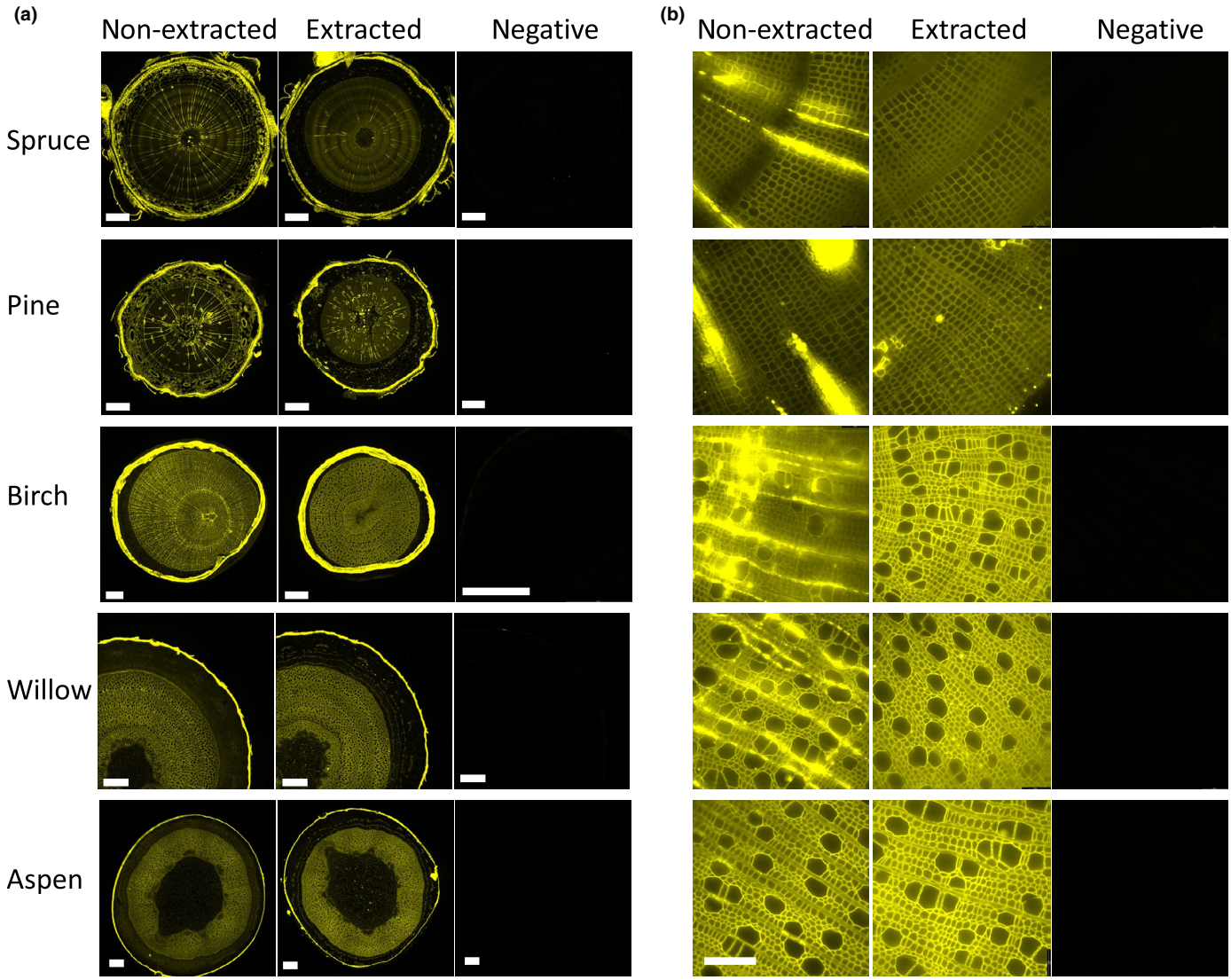

Fig. 4 Histochemical analysis of aliphatic compounds in extracted and nonextracted wood sections of different tree species. Samples collected during dormancy and stained with FY088. (a) Fluorescence channel pictures. Bars, 500 µm. Negative control without FY088 shows signal from lignin autofluorescence. (b) Fluorescence channel pictures at a higher magnification showing wood. Bar, 100 µm, for all micrographs.

expressing *AnAgu67A* under the control of a wood-specific promoter (Ratke *et al.*, 2015) were constructed in *A. thaliana* and their secondarily thickened hypocotyl sections were stained with FY088 before and after removal of extractives. Two independent most highly expressing lines, 2j2 and 5b2, each exhibiting α-glucuronidase activity (Fig. S7a–c), showed the mobilization of FY088-stained toluene-ethanol-resistant lipids from the cell walls of secondary xylem (Figs 3c,d, S7d), similar to transgenic aspen.

To determine whether the mobilization of suberin-like lipids is mediated by the reduction in mGlcA decorations on the xylan backbone or the presence of α-glucuronidase activity in the cell walls, we analyzed the extraction-resistant lipids by FY088 staining in the *gux1gux2* mutant (deficient in the main xylan glucuronosyl transferases responsible for secondary wall xylan glucuronosylation; Mortimer *et al.*, 2010), which under our conditions exhibited *c.* fourfold reduction in xylan glucuronosylation level (Chong *et al.*, 2014). The mutant displayed reduced levels of solvent-resistant aliphatic compounds in the cell walls, whereas its total aliphatic compound levels were unaffected (Figs 3c,d, S7d), indicating increased mobility of cell wall lipids compared with WT (Col-0). Thus, the solvent-resistant suberin-like fraction is dependent on the presence of mGlcA decorations on xylan.

Presence of aliphatic compounds in different woody species

The presence of aliphatic, solvent-resistant compounds in the cell walls of healthy xylem tissue has not been previously recognized in woody species. Therefore, we investigated whether such compounds could be detected in softwoods (Norway spruce (*Picea abies* L.) and Scots pine (*Pinus sylvestris* L.)) and in other hardwoods (downy birch (*Betula pubescens* Ehrh.), goat willow (*Salix caprea* L.), and European aspen (*P. tremula* L.)). Wood samples collected during winter dormancy were sectioned and stained

© 2023 The Authors
New Phytologist © 2023 New Phytologist Foundation

14698137, 2023, 1, Downloaded from https://nph.onlinelibrary.wiley.com/doi/10.1111/nph.18712 by Swedish University Of Agricultural Sciences, Wiley Online Library on [24/04/2023]. See the Terms and Conditions (https://onlinelibrary.wiley.com/terms-and-conditions) on Wiley Online Library for rules of use; OA articles are governed by the applicable Creative Commons License

with FY088 before and after the removal of extractives. In both extracted and nonextracted wood sections, strong, specific staining was observed in the cell walls of mature wood and cork (Fig. 4a,b). Nonextracted samples showed additional signals from live ray cells and resin canals, corresponding to lipids stored for winter dormancy and resin, respectively. The disappearance of these signals in extracted sections confirmed the effective removal of wood extractives (Fig. 4b). Quantification of the FY088 signal in the cell walls (Fig. S8) demonstrated weaker staining in spruce and pine cell walls compared with that observed in the hardwoods. Moreover, the wood of pine, birch, and willow exhibited stronger signals after removal of extractives, suggesting the presence interfering or masking compounds in the extractives. The signal remaining in cell walls after extractives removal corresponding to wall-bound lipids could be clearly seen in all analyzed species.

To analyze the distribution of these lipids in different wood cell wall layers, we examined normal and reaction woods (tension and compression woods) in all studied species at a higher resolution (Fig. 5). In spruce and pine, the solvent-resistant FY088 signals were distributed evenly throughout the primary and secondary wall layers of normal and compression woods, but were weaker in the compression wood. In birch, willow, and aspen, the signals were associated with lignified cell wall layers of normal and tension woods and were excluded from nonlignified gelatinous cell wall layers.

Discussion

Aspergillus niger α-glucuronidase *An*Agu67A was shown to hydrolyze only mGlcA xylan decorations exposed at the nonreducing xylan end, typical to GH67 family of α-glucuronidases. When expressed in hybrid aspen and targeted to cell walls, it could remove *c.* 30% of mGlcA decorations. *Ptxt*Xyn10A xylan endotransglycosylase is the only known GH10 family gene expressed in developing wood that could expose mGlcA for *An*Agu67A hydrolysis (Derba-Maceluch *et al.*, 2015). GH10 enzymes were not analyzed for their ability to hydrolyze the xylan backbone at Xyl*p* residues carrying mGlcA covalently linked to lignin, but it is rather unlikely that such bulky molecules could fit in the binding pocket at their +1 subsite. Therefore, we assume that *Ptxt*Xyn10A cleaves the xylan backbone beside unbound mGlcA. Moreover, as the catalytic site of the GH67 α-glucuronidase of *Cellvibrio japonicus* has been shown to interact with the mGlcA carboxyl residue (Nagy *et al.*, 2003), *An*Agu67A is also predicted to remove only unbound mGlcA xylan decorations; this would affect γ-ester linkages to lignin if these linkages are formed in the cell wall. However, if the γ-ester linkages are formed intracellularly, then their frequency is not expected to be affected by cell wall-localized *An*Agu67A. As we found no reduction in the presence of γ-ester linkages in transgenic aspen lines with a 30% reduction in mGlcA, and no decrease in amount of xylan associated to lignin by either methanolysis-TMS or by NMR analyses, we propose that these linkages are formed intracellularly. The process could be envisioned as an intracellular addition of benzyl substitutions to UDP-linked GlcA, analogous to the addition of ferulate or *p*-coumarate substitutions on UDP-linked arabinose by BAHD family acyl transferases, followed by the incorporation of acylated sugar units to the xylan backbone, as is suggested for grasses (Piston *et al.*, 2010; Bartley *et al.*, 2013; Rennie & Scheller, 2014; Buanafina *et al.*, 2016; Feijao *et al.*, 2022). The intracellular γ-ester linkages formation suggested by the results of this study is in agreement of the recent computational analysis of LCC formation showing that glucuronic acid is less likely to be involved in the nucleophilic attack on quinone methide intermediate compared with neutral sugars or water; thus, it is unlikely to participate in LCC formation in cell walls (Beck *et al.*, 2022). As *An*Agu67A did not affect γ-ester linkages, we did not detect any positive effect of removal of mGlcA on saccharification in transgenic lines.

Our results showed that introducing α-glucuronidase to secondary cell walls or mutating *GUX1* and *GUX2* (encoding the main GlcA transferases involved in secondary wall xylan biosynthesis; Mortimer *et al.*, 2010, 2015; Lee *et al.*, 2012; Rennie *et al.*, 2012; Bromley *et al.*, 2013), both increased the solubility of the suberin-like aliphatic compounds, indicating that glucuronoxylan with mGlcA decorations is involved in anchoring them to wood cell walls. In agreement, no FY088 staining was detected in the gelatinous layers that contain little or no glucuronoxylan (Gorshkova *et al.*, 2015; Guedes *et al.*, 2017). Monomers of cutin and suberin are commonly present in wood extractives, which constitute 1–5% of the dry wood weight (Björklund Jansson & Nilvebrant, 2009) and we extracted more such monomers from transgenic plants expressing *An*Agu67A compared with WT. Suberin monomers have also been identified in the xylem sap of several angiosperm species (Schenk *et al.*, 2021). Wood extractives are known to permeate cell walls in heartwood, which makes them resistant to solvents, suggesting their polymerization and/or covalent linking with other cell wall polymers (Björklund Jansson & Nilvebrant, 2009; Donaldson *et al.*, 2019). Present data suggest their linking to cell walls *via* mGlcA xylan decorations.

The suberin has been shown to remain in the wood cell wall after refluxing wood with lipid solvents (Pearce & Holloway, 1984), although this was previously only thought to occur in infected or damaged wood tissue (Biggs, 1987; Pearce, 1990; Kashyap *et al.*, 2022). Suberin was also demonstrated in cells adjacent to epithelial cells of resin canals in pine (Donaldson *et al.*, 2015). Low suberin levels (0.2–1% of the dry wood weight) were also reported in healthy oak wood, but it was thought to be associated with tyloses or with the inner cell wall layer of tracheary elements, based on Sudan IV and FM1-43 staining patterns (Pearce & Holloway, 1984; Biggs, 1987; Schenk *et al.*, 2021), whereas we identified lipids in all lignified cell wall layers, including the compound middle lamella and the secondary wall layers, using FY088. Sudan IV and FM1-43 are larger than FY088, and may not be able to penetrate more compact and heavily lignified outermost cell wall layers (Ruel *et al.*, 2006; Donaldson *et al.*, 2019) explaining their contrasting labeling pattern compared with FY088. The FY088 labeling pattern is supported by previous time-of-flight secondary ion mass spectrometry imaging, detecting FAs, and DMGs/TMGs in the entire cell wall of tracheids in larch (Fu *et al.*, 2018).

© 2023 The Authors
New Phytologist © 2023 New Phytologist Foundation

14698137, 2023, 1, Downloaded from https://nph.onlinelibrary.wiley.com/doi/10.1111/nph.18712 by Swedish University Of Agricultural Sciences, Wiley Online Library on [24/04/2023]. See the Terms and Conditions (https://onlinelibrary.wiley.com/terms-and-conditions) on Wiley Online Library for rules of use; OA articles are governed by the applicable Creative Commons License

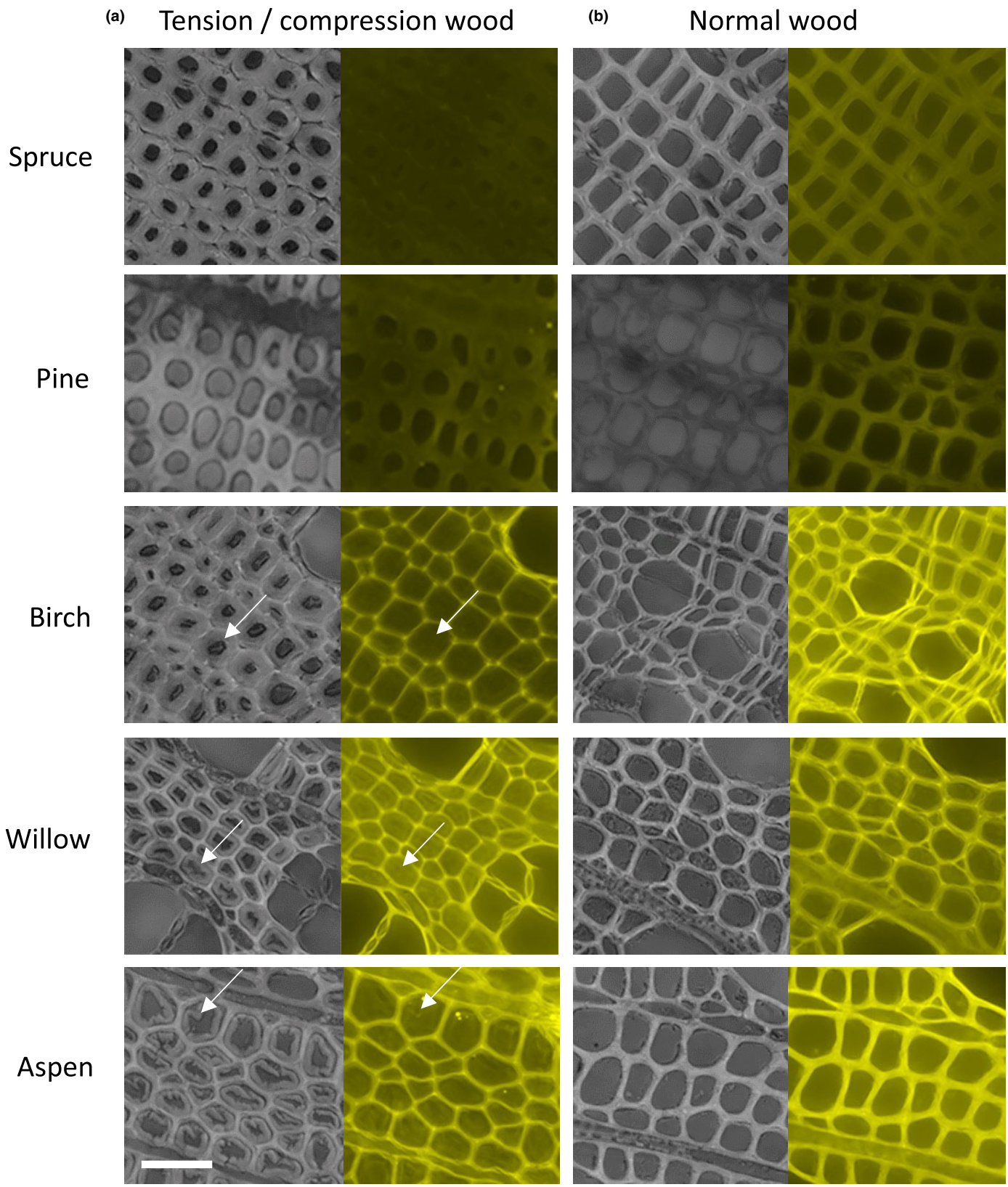

Fig. 5 Histochemical analysis of aliphatic compounds in extracted normal and reaction wood sections of different tree species. Samples collected during dormancy and stained with FY088. (a) Tension or compression wood. (b) Normal wood. Bright field (left) and fluorescence (right) channel pictures. Note the lack of signal in gelatinous cell wall layers (arrows). Bar, 25 μm.

© 2023 The Authors
New Phytologist © 2023 New Phytologist Foundation

14698137, 2023, 1, Downloaded from https://nph.onlinelibrary.wiley.com/doi/10.1111/nph.18712 by Swedish University Of Agricultural Sciences, Wiley Online Library on [24/04/2023]. See the Terms and Conditions (https://onlinelibrary.wiley.com/terms-and-conditions) on Wiley Online Library for rules of use; OA articles are governed by the applicable Creative Commons License

14698137, 2023, 1, Downloaded from https://nph.onlinelibrary.wiley.com/doi/10.1111/nph.18712 by Swedish University Of Agricultural Sciences, Wiley Online Library on [24/04/2023]. See the Terms and Conditions (https://onlinelibrary.wiley.com/terms-and-conditions) on Wiley Online Library for rules of use; OA articles are governed by the applicable Creative Commons License

Future studies should focus on elucidating the structure of these suberin-like components of wood cell walls and their connection to xylan mGlcA. The awareness of the presence of such compounds in wood cell walls is crucial for our understanding of wood physiology, particularly water conduction and wood decay processes. It has also bearing on the utilization of lignocellulose as a renewable resource, for developing novel technological processes of cell wall disintegration, and for solving problems of pitch on machinery observed during wood processing (Back & Allen, 2000).

Acknowledgements

We wish to thank Dr J. Takahashi-Schmidt of the Biopolymer Analytical Platform of KBC at Umeå University for her help with the cell wall analyses; Dr A. Gorzsás of the Vibrational Spectroscopy Core Facility of KBC at Umeå University for his help with the FT-IR analyses; and the Umeå Plant Science Centre (UPSC) Microscopy Facility. We are grateful to Prof. M. Tenkanen, University of Helsinki for the donation of the enzyme substrates and mGlcA. This work was supported by grants from the Knut and Alice Wallenberg Foundation (KAW), the Swedish Governmental Agency for Innovation Systems (VINNOVA), the Swedish Foundation for Strategic Research (SSF; project ValueTree RBP14-0011), Kempestiftelserna, the Swedish Research Council VR, FORMAS, Bio4Energy, the Swedish University of Agricultural Sciences (SLU), Genome Canada, and Genome Quebec.

Competing interests

None declared.

Author contributions

MD-M, ERM and EJM designed the experiments. MD-M conducted most of the experiments with help from the other co-authors. MH performed NMR analyses. AT, JP and ERM identified, cloned, and characterized the *An*Agu67A of *A. niger*. XL conducted the initial glasshouse phenotyping of transgenic aspen lines; MLG and LJJ analyzed the saccharification of transgenic wood. FRB characterized the transgenic *Arabidopsis* lines expressing *AnAgu67A*. MM, INA and TM analyzed the phenolics and lipids extracted from the wood. END and JU conducted the transcriptomic analysis of transgenic aspen. MD-M and EJM wrote the manuscript with help from the co-authors. All the authors read and commented on the manuscript.

ORCID

Ilka N. Abreu https://orcid.org/0000-0003-4728-0161
Félix R. Barbut https://orcid.org/0000-0001-5395-6776
Marta Derba-Maceluch https://orcid.org/0000-0002-8034-3630
Evgeniy N. Donev https://orcid.org/0000-0002-7279-0481
Madhavi L. Gandla https://orcid.org/0000-0003-2798-6298
Mattias Hedenström https://orcid.org/0000-0002-0903-6662
Leif J. Jönsson https://orcid.org/0000-0003-3866-0111
Xiaokun Liu https://orcid.org/0000-0002-4889-8361
Emma R. Master https://orcid.org/0000-0002-6837-9817
Ewa J. Mellerowicz https://orcid.org/0000-0001-6817-1031
Madhusree Mitra https://orcid.org/0000-0002-8653-8770
Thomas Moritz https://orcid.org/0000-0002-4258-3190
Adrian Tsang https://orcid.org/0000-0002-5892-4797
János Urbancsok https://orcid.org/0000-0003-3237-6806

Data availability

The data supporting the findings of this study are available within the paper and/or its Supporting Information. RNA sequencing data are available at ENA (https://www.ebi.ac.uk/ena/browser/home) under accession number: PRJEB53456.

References

Abreu IN, Johansson AI, Sokołowska K, Niittylä T, Sundberg B, Hvidsten TR, Street NR, Moritz T. 2020. A metabolite roadmap of the wood-forming tissue in *Populus tremula*. *New Phytologist* **228**: 1559–1572.

Addison B, Stengel D, Bharadwaj VS, Happs RM, Doeppke C, Wang T, Bomble YJ, Holland GP, Harman-Ware AE. 2020. Selective one-dimensional ^{13}C-^{13}C spin-diffusion solid-state nuclear magnetic resonance methods to probe spatial arrangements in biopolymers including plant cell walls, peptides, and spider silk. *The Journal of Physical Chemistry. B* **124**: 9870–9883.

Back EL, Allen LH. 2000. *Pitch control, wood resin and deresination*. Atlanta, GA, USA: TAPPI Press.

Balakshin M, Capanema E, Gracz H, Chang HM, Jameel H. 2011. Quantification of lignin-carbohydrate linkages with high-resolution NMR spectroscopy. *Planta* **233**: 1097–1110.

Bar-On YM, Phillips R, Milo R. 2018. The biomass distribution on earth. *Proceedings of the National Academy of Sciences, USA* **115**: 6506–6511.

Bartley LE, Peck ML, Kim SR, Ebert B, Manisseri C, Chiniquy DM, Sykes R, Gao L, Rautengarten C, Vega-Sánchez ME *et al.* 2013. Overexpression of a BAHD acyltransferase, *Os*At10, alters rice cell wall hydroxycinnamic acid content and saccharification. *Plant Physiology* **161**: 1615–1633.

Beck S, Choi P, Mushrif SH. 2022. Origins of covalent linkages within the lignin-carbohydrate network of biomass. *Physical Chemistry Chemical Physics* **24**: 20480–20490.

Berglund J, Mikkelsen D, Flanagan BM, Dhital S, Gaunitz S, Henriksson G, Lindström ME, Yakubov GE, Gidley MJ, Vilaplana F. 2020. Wood hemicelluloses exert distinct biomechanical contributions to cellulose fibrillar networks. *Nature Communications* **11**: 4692.

Bernards MA. 2002. Demystifying suberin. *Canadian Journal of Botany* **80**: 227–240.

Biggs AR. 1987. Occurrence and location of suberin in wound reaction zones in xylem of 17 tree species. *Phytopathology* **77**: 718–725.

Björklund Jansson M, Nilvebrant N-O. 2009. Wood extractives. In: Ek M, Gellerstedt G, Henriksson G, eds. *Wood chemistry and wood biotechnology*. Berlin, Germany: de Gruyter, 147–171.

Bromley JR, Busse-Wicher M, Tryfona T, Mortimer JC, Zhang Z, Brown DM, Dupree P. 2013. GUX1 and GUX2 glucuronyltransferases decorate distinct domains of glucuronoxylan with different substitution patterns. *The Plant Journal* **74**: 423–434.

Buanafina MM, Fescemyer HW, Sharma M, Shearer EA. 2016. Functional testing of a PF02458 homologue of putative rice arabinoxylan feruloyl transferase genes in *Brachypodium distachyon*. *Planta* **243**: 659–674.

Busse-Wicher M, Gomes TC, Tryfona T, Nikolovski N, Stott K, Grantham NJ, Bolam DN, Skaf MS, Dupree P. 2014. The pattern of xylan acetylation suggests xylan may interact with cellulose microfibrils as a twofold helical screw

© 2023 The Authors
New Phytologist © 2023 New Phytologist Foundation

in the secondary plant cell wall of *Arabidopsis thaliana*. *The Plant Journal* **79**: 492–506.

Busse-Wicher M, Li A, Silveira RL, Pereira CS, Tryfona T, Gomes TC, Skaf MS, Dupree P. 2016. Evolution of xylan substitution patterns in gymnosperms and angiosperms: implications for xylan interaction with cellulose. *Plant Physiology* **171**: 2418–2431.

Chang SJ, Puryear J, Cairney J. 1993. A simple and efficient method for isolating RNA from pine trees. *Plant Molecular Biology Reporter* **11**: 113–116.

Chong SL, Derba-Maceluch M, Koutaniemi S, Gómez LD, McQueen-Mason SJ, Tenkanen M, Mellerowicz EJ. 2015. Active fungal GH115 α-glucuronidase produced in *Arabidopsis thaliana* affects only the UX1-reactive glucuronate decorations on native glucuronoxylans. *BMC Biotechnology* **15**: 56.

Chong SL, Koutaniemi S, Virkki L, Pynnönen H, Tuomainen P, Tenkanen M. 2013. Quantitation of 4-*O*-methylglucuronic acid from plant cell walls. *Carbohydrate Polymers* **91**: 626–630.

Chong SL, Virkki L, Maaheimo H, Juvonen M, Derba-Maceluch M, Koutaniemi S, Roach M, Sundberg B, Tuomainen P, Mellerowicz EJ *et al.* 2014. *O*-acetylation of glucuronoxylan in *Arabidopsis thaliana* wild type and its change in xylan biosynthesis mutants. *Glycobiology* **24**: 494–506.

Clough SJ, Bent AF. 1998. Floral dip: a simplified method for *Agrobacterium* mediated transformation of *Arabidopsis thaliana*. *The Plant Journal* **16**: 735–743.

Correia VG, Bento A, Pais J, Rodrigues R, Haliński ŁP, Frydrych M, Greenhalgh A, Stepnowski P, Vollrath F, King AWT *et al.* 2020. The molecular structure and multifunctionality of the cryptic plant polymer suberin. *Materials Today Bio* **5**: 100039.

Derba-Maceluch M, Awano T, Takahashi J, Lucenius J, Ratke C, Kontro I, Busse-Wicher M, Kosik O, Tanaka R, Winzéll A *et al.* 2015. Suppression of xylan endotransglycosylase *Ptxt*Xyn10A affects cellulose microfibril angle in secondary wall in aspen wood. *New Phytologist* **205**: 666–681.

Donaldson LA, Nanayakkara B, Radotić K, Djikanovic-Golubović D, Mitrović A, Bogdanović Pristov J, Simonović Radosavljević J, Kalauzi A. 2015. Xylem parenchyma cell walls lack a gravitropic response in conifer compression wood. *Planta* **242**: 1413–1424.

Donaldson LA, Singh A, Raymond L, Hill S, Schmitt U. 2019. Extractive distribution in *Pseudotsuga menziesii*: effects on cell wall porosity in sapwood and heartwood. *IAWA Journal* **40**: 721–740.

Feijao C, Morreel K, Anders N, Tryfona T, Busse-Wicher M, Kotake T, Boerjan W, Dupree P. 2022. Hydroxycinnamic acid-modified xylan side chains and their cross-linking products in rice cell walls are reduced in the xylosyl arabinosyl substitution of xylan 1 mutant. *The Plant Journal* **109**: 1152–1167.

Fernandes AN, Thomas LH, Altaner CM, Callow P, Forsyth VT, Apperley DC, Kennedy CJ, Jarvis MC. 2011. Nanostructure of cellulose microfibrils in spruce wood. *Proceedings of the National Academy of Sciences, USA* **108**: E1195–E1203.

Franková L, Fry SC. 2011. Phylogenetic variation in glycosidases and glycanases acting on plant cell wall polysaccharides, and the detection of transglycosidase and trans-β-xylanase activities. *The Plant Journal* **67**: 662–681.

Fu T, Elie N, Brunelle A. 2018. Radial distribution of wood extractives in European larch *Larix decidua* by TOF-SIMS imaging. *Phytochemistry* **150**: 31–39.

Gandla LM, Derba-Maceluch M, Liu X, Gerber L, Master ER, Mellerowicz EJ, Jönsson LJ. 2015. Expression of a fungal glucuronoyl esterase in *Populus*: effects on wood properties and saccharification efficiency. *Phytochemistry* **112**: 210–220.

Gerber L, Eliasson M, Trygg J, Moritz T, Sundberg B. 2012. Multivariate curve resolution provides a high-throughput data processing pipeline for pyrolysis gas chromatography/mass spectrometry. *Journal of Analytical and Applied Pyrolysis* **95**: 95–100.

Giummarella N, Pu Y, Ragauskas AJ, Lawoko M. 2019. A critical review on the analysis of lignin carbohydrate bonds. *Green Chemistry* **21**: 1573–1595.

Gorshkova T, Mokshina N, Chernova T, Ibragimova N, Salnikov V, Mikshina P, Tryfona T, Banasiak A, Immerzeel P, Dupree P *et al.* 2015. Aspen tension wood fibers contain β-(1→4)-galactans and acidic arabinogalactans retained by cellulose microfibrils in gelatinous walls. *Plant Physiology* **169**: 2048–2063.

Graça J. 2010. Hydroxycinnamates in suberin formation. *Phytochemistry Reviews* **9**: 85–91.

Grantham NJ, Wurman-Rodrich J, Terrett OM, Lyczakowski JJ, Stott K, Iuga D, Simmons TJ, Durand-Tardif M, Brown SP, Dupree R *et al.* 2017. An even pattern of xylan substitution is critical for interaction with cellulose in plant cell walls. *Nature Plants* **3**: 859–865.

Gray-Mitsumune M, Mellerowicz EJ, Abe H, Schrader J, Winzéll A, Sterky F, Blomqvist K, McQueen-Mason S, Teeri TT, Sundberg B. 2004. Expansins abundant in secondary xylem belong to subgroup A of the α-expansin gene family. *Plant Physiology* **135**: 1552–1564.

Gray-Mitsumune M, Mellerowicz EJ, Abe H, Schrader J, Winzéll A, Sterky F, Blomqvist K, McQueen-Mason S, Teeri TT, Sundberg B. 2008. Ectopic expression of a wood-abundant expansin PttEXPA1 promotes cell expansion in primary and secondary tissues in aspen. *Plant Biotechnology Journal* **6**: 62–72.

Guedes FTP, Laurans F, Quemener B, Assor C, Lainé-Prade V, Boizot N, Vigouroux J, Lesage-Descauses MC, Leplé JC, Déjardin A *et al.* 2017. Non-cellulosic polysaccharide distribution during G-layer formation in poplar tension wood fibers: abundance of rhamnogalacturonan I and arabinogalactan proteins but no evidence of xyloglucan. *Planta* **246**: 857–878.

Gullberg J, Jonsson P, Nordström A, Sjöström M, Moritz T. 2004. Design of experiments: an efficient strategy to identify factors influencing extraction and derivatization of *Arabidopsis thaliana* samples in metabolomic studies with gas chromatography/mass spectrometry. *Analytical Biochemistry* **331**: 283–295.

Hedenström M, Wiklund-Lindström S, Oman T, Lu F, Gerber L, Schatz P, Sundberg B, Ralph J. 2009. Identification of lignin and polysaccharide modifications in *Populus* wood by chemometric analysis of 2D NMR spectra from dissolved cell walls. *Molecular Plant* **2**: 933–942.

Kang X, Kirui A, Dickwella Widanage MC, Mentink-Vigier F, Cosgrove DJ, Wang T. 2019. Lignin-polysaccharide interactions in plant secondary cell walls revealed by solid-state NMR. *Nature Communications* **10**: 1–9.

Karimi M, Inzé D, Depicker A. 2002. Gateway vectors for *Agrobacterium*-mediated plant transformation. *Trends in Plant Science* **7**: 193–195.

Kashyap A, Jiménez-Jiménez ÁL, Zhang W, Capellades M, Srinivasan S, Laromaine A, Serra O, Figueras M, Rencoret J, Gutiérrez A *et al.* 2022. Induced ligno-suberin vascular coating and tyramine-derived hydroxycinnamic acid amides restrict *Ralstonia solanacearum* colonization in resistant tomato. *New Phytologist* **234**: 1411–1429.

Kasper PT, Rojas-Chertó M, Mistrik R, Reijmers T, Hankemeier T, Vreeken RJ. 2012. Fragmentation trees for the structural characterisation of metabolites. *Rapid Communications in Mass Spectrometry* **26**: 2275–2286.

Kim H, Ralph J, Akiyama T. 2008. Solution-state 2D NMR of ball-milled plant cell wall gels in DMSO-d6. *Bioenergy Research* **1**: 56–66.

Koutaniemi S, Guillon F, Tranquet O, Bouchet B, Tuomainen P, Virkki L, Petersen HL, Willats WG, Saulnier L, Tenkanen M. 2012. Substituent-specific antibody against glucuronoxylan reveals close association of glucuronic acid and acetyl substituents and distinct labeling patterns in tree species. *Planta* **236**: 739–751.

Kumar V, Hainaut M, Delhomme N, Mannapperuma C, Immerzeel P, Street NR, Henrissat B, Mellerowicz EJ. 2019. Poplar carbohydrate-active enzymes: whole-genome annotation and functional analyses based on RNA expression data. *The Plant Journal* **99**: 598–609.

Lee C, Teng Q, Zhong R, Ye ZH. 2012. Arabidopsis GUX proteins are glucuronyltransferases responsible for the addition of glucuronic acid side chains onto xylan. *Plant & Cell Physiology* **53**: 1204–1216.

Lee C, Teng Q, Zhong R, Ye ZH. 2014. Alterations of the degree of xylan acetylation in *Arabidopsis* xylan mutants. *Plant Signaling & Behavior* **9**: 1186–1199.

Livak KJ, Schmittgen TD. 2001. Analysis of relative gene expression data using real-time quantitative PCR and the $2^{-\Delta\Delta CT}$ method. *Methods* **25**: 402–408.

Lux A, Morita S, Abe J, Ito K. 2005. An improved method for clearing and staining free-hand sections and whole-mount samples. *Annals of Botany* **96**: 989–996.

Lyczakowski JJ, Bourdon M, Terrett OM, Helariutta Y, Wightman R, Dupree P. 2019. Structural imaging of native cryo-preserved secondary cell walls reveals the presence of macrofibrils and their formation requires normal cellulose, lignin and xylan biosynthesis. *Frontiers in Plant Science* **10**: 1398.

Lyczakowski JJ, Wicher KB, Terrett OM, Faria-Blanc N, Yu X, Brown D, Krogh KBRM, Dupree P, Busse-Wicher M. 2017. Removal of glucuronic acid

© 2023 The Authors
New Phytologist © 2023 New Phytologist Foundation

14698137, 2023, 1, Downloaded from https://nph.onlinelibrary.wiley.com/doi/10.1111/nph.18712 by Swedish University Of Agricultural Sciences, Wiley Online Library on [24/04/2023]. See the Terms and Conditions (https://onlinelibrary.wiley.com/terms-and-conditions) on Wiley Online Library for rules of use; OA articles are governed by the applicable Creative Commons License

from xylan is a strategy to improve the conversion of plant biomass to sugars for bioenergy. *Biotechnology for Biofuels* **10**: 224.

Lyczakowski JJ, Yu L, Terrett OM, Fleischmann C, Temple H, Thorlby G, Sorieul M, Dupree P. 2021. Two conifer GUX clades are responsible for distinct glucuronic acid patterns on xylan. *New Phytologist* **231**: 1720–1733.

Martínez-Abad A, Berglund J, Toriz G, Gatenholm P, Henriksson G, Lindström M, Wohlert J, Vilaplana F. 2017. Regular motifs in xylan modulate molecular flexibility and interactions with cellulose surfaces. *Plant Physiology* **175**: 1579–1592.

Martínez-Abad A, Giummarella N, Lawoko M, Vilaplana F. 2018. Differences in extractability under subcritical water reveal interconnected hemicellulose and lignin recalcitrance in birch hardwoods. *Green Chemistry* **20**: 2534–2546.

Martínez-Abad A, Jiménez-Quero A, Wohlert J. 2020. Influence of the molecular motifs of mannan and xylan populations on their recalcitrance and organization in spruce softwoods. *Green Chemistry* **22**: 3956–3970.

Melo T, Figueiredo ARP, da Costa E, Couto D, Silva J, Domingues MR, Domingues P. 2021. Ethanol extraction of polar lipids from *Nannochloropsis oceanica* for food, feed, and biotechnology applications evaluated using lipidomic approaches. *Marine Drugs* **19**: 593.

Meshitsuka G, Nakano J. 1977. Studies on the mechanism of lignin color reaction XI. Maüle color reaction. *Mokuzai Gakkaishi* **23**: 232–236.

Mortimer JC, Faria-Blanc N, Yu X, Tryfona T, Sorieul M, Ng YZ, Zhang Z, Stott K, Anders N, Dupree P. 2015. An unusual xylan in *Arabidopsis* primary cell walls is synthesised by GUX3, IRX9L, IRX10L and IRX14. *The Plant Journal* **83**: 413–426.

Mortimer JC, Miles GP, Brown DM, Zhang Z, Segura MP, Weimar T, Yu X, Seffen KA, Stephens E, Turner SR *et al.* 2010. Absence of branches from xylan in *Arabidopsis gux* mutants reveals potential for simplification of lignocellulosic biomass. *Proceedings of the National Academy of Sciences, USA* **107**: 17409–17414.

Nagy T, Nurizzo D, Davies GJ, Biely P, Lakey JH, Bolam DN, Gilbert HJ. 2003. The alpha-glucuronidase, GlcA67A, of *Cellvibrio japonicus* utilizes the carboxylate and methyl groups of aldobiouronic acid as important substrate recognition determinants. *The Journal of Biological Chemistry* **278**: 20286–20292.

Naseer S, Lee Y, Lapierre C, Franke R, Nawrath C, Geldner N. 2012. Casparian strip diffusion barrier in *Arabidopsis* is made of a lignin polymer without suberin. *Proceedings of the National Academy of Sciences, USA* **109**: 10101–10106.

Öman T, Tessem MB, Bathen TF, Bertilsson H, Angelsen A, Hedenström M, Andreassen T. 2014. Identification of metabolites from 2D ^{1}H-^{13}C HSQC NMR using peak correlation plots. *BMC Bioinformatics* **15**: 413.

Pawar PM, Derba-Maceluch M, Chong SL, Gómez LD, Miedes E, Banasiak A, Ratke C, Gaertner C, Mouille G, McQueen-Mason SJ *et al.* 2016. Expression of fungal acetyl xylan esterase in *Arabidopsis thaliana* improves saccharification of stem lignocellulose. *Plant Biotechnology Journal* **14**: 387–397.

Pearce RB. 1990. Occurrence of decay-associated xylem suberization in a range of woody species. *European Journal of Forest Pathology* **20**: 275–289.

Pearce RB, Holloway PJ. 1984. Suberin in the sapwood of oak (*Quercus robur* L.): its composition from a compartmentalization barrier and its occurrence in tyloses in undecayed wood. *Physiological Plant Pathology* **24**: 71–81.

Pereira CS, Silveira RL, Dupree P, Skaf MS. 2017. Effects of xylan side-chain substitutions on xylan–cellulose interactions and implications for thermal pretreatment of cellulosic biomass. *Biomacromolecules* **18**: 1311–1321.

Pfaffl MW. 2001. A new mathematical model for relative quantification in real-time RT-PCR. *Nucleic Acids Research* **29**: e45.

Piston F, Uauy C, Fu L, Langston J, Labavitch J, Dubcovsky J. 2010. Down-regulation of four putative arabinoxylan feruloyl transferase genes from family PF02458 reduces ester-linked ferulate content in rice cell walls. *Planta* **231**: 677–691.

Ratke C, Pawar PM, Balasubramanian VK, Naumann M, Duncranz ML, Derba-Maceluch M, Gorzsás A, Endo S, Ezcurra I, Mellerowicz EJ. 2015. Populus GT 43 family members group into distinct sets required for primary and secondary wall xylan biosynthesis and include useful promoters for wood modification. *Plant Biotechnology Journal* **13**: 26–37.

Rennie EA, Hansen SF, Baidoo EE, Hadi MZ, Keasling JD, Scheller HV. 2012. Three members of the Arabidopsis glycosyltransferase family 8 are xylan glucuronosyltransferases. *Plant Physiology* **159**: 1408–1417.

Rennie EA, Scheller HV. 2014. Xylan biosynthesis. *Current Opinion in Biotechnology* **26**: 100–107.

Rudsander UJ, Denman S, Raza S, Teeri TT. 2003. Molecular features of family GH9 cellulases in hybrid aspen and the filamentous fungus *Phanerochaete chrysosporium*. *Journal of Applied Glycoscience* **50**: 253–256.

Ruel K, Chevalier-Billosta V, Guillemin F, Sierra JB, Joseleau J-P. 2006. The wood cell wall at the ultrastructural scale- formation and topochemical organization. *Maderas Ciencia y Tecnología* **8**: 107–116.

Schenk HJ, Michaud JM, Mocko K, Espino S, Melendres T, Roth MR, Welti R, Kaack L, Jansen S. 2021. Lipids in xylem sap of woody plants across the angiosperm phylogeny. *The Plant Journal* **105**: 1477–1494.

Shakeri Yekta S, Hedenström M, Svensson BH, Sundgren I, Dario M, Enrich-Prast A, Hertkorn N, Björn A. 2019. Molecular characterization of particulate organic matter in full scale anaerobic digesters: an NMR spectroscopy study. *Science of the Total Environment* **685**: 1107–1115.

Storms R, Zheng Y, Li H, Sillaots S, Martinez-Perez A, Tsang A. 2005. Plasmid vectors for protein production, gene expression and molecular manipulations in *Aspergillus niger*. *Plasmid* **53**: 191–204.

Tarasov D, Leitch M, Fatehi P. 2018. Lignin–carbohydrate complexes: properties, applications, analyses, and methods of extraction: a review. *Biotechnology for Biofuels* **11**: 269.

Tenkanen M, Siika-aho M. 2000. An alpha-glucuronidase of *Schizophyllum commune* acting on polymeric xylan. *Journal of Biotechnology* **78**: 149–161.

Terashima N, Kitano K, Kojima M, Yoshida M, Yamamoto H, Westermark U. 2009. Nanostructural assembly of cellulose, hemicellulose, and lignin in the middle layer of secondary wall of ginkgo tracheid. *Journal of Wood Science* **55**: 409–416.

Terrett OM, Dupree P. 2019. Covalent interactions between lignin and hemicelluloses in plant secondary cell walls. *Current Opinion in Biotechnology* **56**: 97–104.

Terrett OM, Lyczakowski JJ, Yu L, Iuga D, Franks WT, Brown SP, Dupree R, Dupree P. 2019. Molecular architecture of softwood revealed by solid-state NMR. *Nature Communications* **10**: 4978.

Theander O, Westerlund EA. 1986. Studies on dietary fiber. 3. Improved procedures for analysis of dietary fiber. *Journal of Agricultural and Food Chemistry* **34**: 330–336.

Updegraff D. 1969. Semimicro determination of cellulose in biological materials. *Analytical Biochemistry* **32**: 420–424.

Supporting Information

Additional Supporting Information may be found online in the Supporting Information section at the end of the article.

Fig. S1 Enzymatic activity of recombinant *An*Agu67A purified from *Aspergillus niger* Tiegh.

Fig. S2 Chemical analyses and saccharification sugar yields of wood of transgenic aspen (*Populus tremula* L. × *tremuloides* Michx.) lines ectopically expressing SP_{Cel9B3}*:AnAgu67A*.

Fig. S3 Characterization of transgenic aspen (*Populus tremula* L. × *tremuloides* Michx.) lines carrying *35S::*SP_{Cel9B3}*:AnAgu67A* construct.

Fig. S4 Chemical analysis of dioxane lignin of transgenic and wild-type wood samples extracted with toluene-ethanol.

Fig. S5 NMR spectral characterization of dioxane-extracted lignin without removal of extractives (nonextracted wood) and after extractives removal (extracted wood).

© 2023 The Authors
New Phytologist © 2023 New Phytologist Foundation

14698137, 2023, 1, Downloaded from https://nph.onlinelibrary.wiley.com/doi/10.1111/nph.18712 by Swedish University Of Agricultural Sciences, Wiley Online Library on [24/04/2023]. See the Terms and Conditions (https://onlinelibrary.wiley.com/terms-and-conditions) on Wiley Online Library for rules of use; OA articles are governed by the applicable Creative Commons License

Fig. S6 Histochemical analysis of lipophilic substances in wood with FY088 staining.

Fig. S7 General characterization of transgenic *Arabidopsis* lines carrying *WP::SP*$_{Cel9B3}$*:AnAgu67A* construct.

Fig. S8 Histochemical analysis of aliphatic compounds in cell walls in the wood of different species with FY088 staining.

Methods S1 Gene cloning and recombinant expression of *An*Agu67A.

Methods S2 Enzyme activity of recombinant *An*Agu67A.

Methods S3 Thin-layer chromatography for detecting of *An*Agu67A alpha-glucuronidase activity.

Table S1 Primers used for RT-PCR analyses and cloning of hybrid genes for expression vectors.

Table S2 Differentially expressed genes in developing wood of transgenic aspen (*Populus tremula* L. × *tremuloides* Michx.) lines 4 and 6 expressing *SP*$_{Cel9B3}$*:AnAgu67A* compared with wild-type.

Table S3 List of lipidomics peaks (Mass@retention time) detected in wood extracts by liquid chromatography–mass spectrometry in positive and negative modes and analysis of differences in their integrated signal intensities between transgenic and wild-type samples by *t*-test.

Table S4 List of identified lipidic compounds in wood extracts that differed in abundance between transgenic and wild-type samples.

Table S5 List of all signals from metabolomics analysis.

Table S6 List of identified phenolic compounds in wood extracts that differed in abundance between transgenic and wild-type samples.

Please note: Wiley is not responsible for the content or functionality of any Supporting Information supplied by the authors. Any queries (other than missing material) should be directed to the *New Phytologist* Central Office.

See also the Commentary on this article by Oliveira, **238**: 8–10.

© 2023 The Authors
New Phytologist © 2023 New Phytologist Foundation

14698137, 2023, 1, Downloaded from https://nph.onlinelibrary.wiley.com/doi/10.1111/nph.18712 by Swedish University Of Agricultural Sciences, Wiley Online Library on [24/04/2023]. See the Terms and Conditions (https://onlinelibrary.wiley.com/terms-and-conditions) on Wiley Online Library for rules of use; OA articles are governed by the applicable Creative Commons License